Bull. Astr. Soc. India (2002) 30, 911–941

Photometric Catalogs of Four EMSS Poor Clusters of Galaxies

Mangala Sharma and T. P. Prabhu
Indian Institute of Astrophysics, Bangalore 560 034, India

Received 17 April 2002; accepted 27 September 2002

Abstract.

We have used the 2.3-meter Vainu Bappu Telescope to perform CCD imaging of X-ray-selected poor clusters of galaxies. Our sample consists of four X-ray luminous clusters in the *Einstein Observatory* Extended Medium Sensitivity Survey (EMSS) and noted by Gioia & Luppino (1994) to be optically less rich than Abell clusters. The sample spans a redshift range of $0.08 \leq z \leq 0.22$. We have assembled catalogs of galaxies detected in the cluster fields to a magnitude limit $m_V \approx 22$. This paper describes the data reduction performed on the CCD images, the methods used to construct the extended object catalogs, the photometric calibrations, and some understanding of their completeness and contamination.

Keywords : galaxies: clusters – galaxies: photometry

1. Introduction

Most galaxies in the universe are members of multi-galaxy systems (pairs, small groups, clusters); fewer than 45% are isolated 'field' galaxies (e.g., Giuricin et al. 2000) and a small 5% reside in the other extremum of dense 'rich' clusters. Galaxy properties, and their chemical and dynamical evolution are sensitive to their environment. Non-isolated galaxies can bear the brunt of several interactions: with other galaxies, with the tidal field of the group or cluster, and with the diffuse, hot ($kT = 3 - 9$keV) X-ray emitting intracluster medium. They then suffer changes in their Hubble type, nuclear and star-formation activities, etc. Environmental variations are tied to system properties such as velocity dispersion, total cluster mass, baryon fraction, galaxy population and density.

Galaxies within rich cluster and compact groups evince the most dramatic environmental forcing relative to their cousins in the field. Since rich clusters are easily detected even to high redshifts, they have been the focus of many detailed studies (see e.g., Dressler 1984). Similarly, compact groups with their extreme spatial densities and low velocity-dispersions have been subjects of much attention and controversy (see review by Hickson 1997). However, comprising only a few percent of the total galaxy population and subject to exceptionally strong environmental effects, the denizens of rich clusters and compact groups represent a minority population.

It is therefore interesting to examine how galaxies evolve in small or 'poor' clusters that are not so massive as rich clusters, but are far more numerous. Such systems form a natural and continuous extension to lower richness, mass, size, and luminosity from the rare rich clusters (see, e.g., Bahcall 1980; White et al. 1999). Hence they contribute a significant quantity to the mass and baryonic fraction of the universe and contain a larger fraction of the galaxy population than do their richer versions. In hierarchical structure formation scenarios, clusters of galaxies are assembled by the merging of smaller systems. Therefore, the well-studied rich clusters are likely to be composed of several poorer systems. Poor clusters bridge the gap between the well-studied environments of the rich clusters and the special groups such as the Hickson Compact Groups. Within poor clusters, in comparison with rich clusters, the effects of the intracluster plasma are comparable but the tidal perturbations due to the global potential are weaker, and in comparison with small groups, the galaxy velocity dispersions are higher and the global potential deeper.

Poor clusters do not proffer themselves to detailed study easily, mainly due to their low relief against the background. Further, as poor systems are best identified and usually studied in our immediate neighborhood (e.g., Beers et al. 1995; Ledlow et al. 1996; Mahdavi et al. 2000; see also review by Mulchaey 2000), remarkably little is known about these systems at intermediate or high redshifts. But local as well as moderately distant poor clusters are crucial for interpretation of systems at high redshift. It is only recently — thanks largely to X-ray surveys that are beginning to detect poor systems at increasingly larger redshifts although their goal is usually to find distant rich clusters (e.g., Scharf et al. 1997; Vikhlinin et al. 1998) — that these entities have started receiving the attention they merit. It is important for statistical studies of groups and poor clusters to develop a broad reach like that of rich cluster studies.

This paper presents optical imaging data on four poor clusters of galaxies at moderate redshifts ($0.08 < z < 0.22$). Four clusters do not comprise a statistically-complete sample. Nevertheless, observations of these poor clusters represent a contribution to the pool of information required for understanding galaxy properties and evolution in different environs. There are several good reasons for using optical observations for our purpose of studying normal galaxies in the not-too-distant universe. Normal galaxies are dominated by starlight, and emit much of their radiation in the visible band. Galaxy colors reveal the spectral energy distributions at a rudimentary level, and can thus shed

light on the stellar composition of faint galaxies; the details, however, can be derived only from spectral lines. At moderate distances ($z \sim 0.25$) the redshifted optical radiation of the galaxies still remains largely in the visible bands. Though galaxy evolution becomes evident even at $z \sim 0.2$ (e.g., Caldwell & Rose 1997), the objects are not so changed that local counterparts cannot be found. Therefore, comparison of colors of intermediate redshift galaxies and local ones does not lead to disastrous inconsistencies. Cosmological corrections to galaxy luminosity and surface brightness are small, and gravitational lensing is not of serious concern at moderate redshifts.

This paper is organized as follows: in §2 we define our sample, and describe the observations. In §3 we list the main features of the CCD data reduction. In §4 we give an account of how we detected and cataloged the objects, and bifurcated them into stellar and extended objects. We then discuss the photometric calibration and astrometry. Following this, we provide the galaxy catalogs and characterize them in terms of their completeness and contamination by stellar objects. In §5 we summarize the properties of the resulting catalog of extended objects in the fields of the poor clusters. The appendices contain the actual catalogs of galaxies in the fields of the four poor clusters we have observed.

2. Sample and Observations

2.1 Definition and Sample

The very definition of poor clusters in the literature is not unique. Generally, a system of galaxies is termed poor if its population *fails* to satisfy some limiting (say, that of Abell 1958) number criterion for a *rich* cluster. Poor clusters span the entire gamut of galaxy populations from the small Hickson Compact Groups, through systems like the Local Group, upto (and including) the threshold of rich clusters.

Poor clusters are difficult to identify through projected or even spatial galaxy overdensity, as their contrast against the background is weak. The observation that over 80% of all rich clusters (richness ≥ 0) are X-ray sources (Briel & Henry 1993) and that about 50% of all nearby groups of galaxies (regardless of whether they are compact or loose) contain a hot intracluster or intragroup medium (e.g., Ponman et al. 1996; Burns et al. 1996) motivates a method of cluster selection in X-ray that is more secure than in the optical. X-ray emission, whose luminosity is proportional to the square of the gas density, implies the presence of a deep potential well — such as that of a massive galaxy system — to trap the high-energy $10^7 K$ plasma.

We have chosen poor clusters based on their X-ray emission and sparse galaxy population in optical images. The poor clusters for which we present photometry here are from the cluster subsample (Gioia & Luppino 1994; henceforth GL94) of the Extended Medium Sensitivity Survey (EMSS; Gioia et al. 1990) catalog of sources discovered serendipitously with the *Einstein* X-ray satellite in the $0.3 - 3.5$ keV energy band. From inspection of

deep CCD images taken as follow-up optical observations, GL94 provide comments about the optical appearance of the clusters and on the spectral properties of the brightest cluster members. GL94 note that nineteen of the approximately one hundred EMSS clusters appear to be "poor", i.e., display morphologies and galaxy counts that are best described as that of poor clusters.

Of these nineteen putative poor clusters, we acquired data for four that show extended X-ray emission of luminosity $L_X \geq 3 \times 10^{43}$ erg s^{-1}in the 0.3–3.5keV band, are at moderate redshifts $0.08 < z < 0.25$, and lie north of declination $\delta \sim -30^0$ for good access from the Vainu Bappu Observatory. A preliminary quantitative richness estimate of the clusters using galaxy counts from the red plates of the Automated Plate Scanner catalogs (Pennington et al. 1993) showed them to be less populated than Abell $R = 1$ clusters at similar redshifts. Table 2.1 presents the major properties of these four poor clusters.

Table 1. Properties of the poor clusters. The columns are (1) cluster name (2) right ascension (J2000), (3) declination (J2000) (4) *Einstein* X-ray luminosity in 10^{44}erg s^{-1}(5) spectroscopic redshift (6) apparent magnitude of the brightest cluster galaxy and (7) the Galactic extinction in the V-band.

Cluster	RA (J2000)	Dec (J2000)	L_X 10^{44}erg s^{-1}	z	M_B mag	A_V mag
MS 0002.8+1556	00:05:25.1	+16:13:24.1	1.64	0.116	16.0	0.158
MS 0301.7+1516	03:04:30.4	+15:27:53.0	0.33	0.083	16.9	0.554
MS 0735.6+7421	07:41:50.1	+74:14:01.4	6.12	0.216	17.7	0.077
MS 1306.7−0121	13:09:18.0	−01:37:21.4	1.70	0.088	16.0	0.094

Although X-ray selection minimizes the chances of spurious detection, the EMSS cluster subsample is not entirely free of selection biases. Recent optical and X-ray follow-up observations have shown that a few (< 5%) clusters are actually misclassified stars or AGN (e.g., Rector et al. 1999). Despite its classification errors, the EMSS cluster catalog remains one of the best sources for genuine clusters selected in X-ray, along with similar projects such as the Wide Angle ROSAT Pointed Survey (Scharf et al. 1997) and the Serendipitous High-Redshift Archival ROSAT Cluster survey (Romer et al. 2000), which are ongoing studies of galaxy clusters detected serendipitously in archival ROSAT observations.

2.2 Imaging Set-Up and Technique

In this work, we use optical images obtained on both photometric and non-photometric nights close to new moon. The following section describes the instruments and imaging techniques we used.

We acquired optical imaging observations at the prime focus of the 2.34-m Vainu Bappu Telescope (VBT), at the Vainu Bappu Observatory (VBO), Kavalur, India. The observatory (longitude 78°.8 E, latitude 12°.5 N, altitude 730m above sea level) is operated by the Indian Institute of Astrophysics, Bangalore. The VBT has a prime focal ratio of f/3.24; for direct imaging this configuration provides an image scale of 26 arcsec/mm, and a field of view of 10.5 arcmin × 10.5 arcmin. We employed the following filters in our observations: broad-band blue, visual, red and near infra-red (approximating the standard B, V, R and I photometric bands). In the span of 4-5 years over which we obtained observations, three sets of broad-band filters were available at the VBT – two sets of circular filters of 2-inch radii and later another set of 3-inch radii. The 2-inch filters are somewhat undersized to cover the entire field of view of the images, and give rise to vignetting in the corners of the CCD frame. We made efforts to obtain observations in all bands for a cluster on the same night; however we were not always successful in achieving this objective.

The camera for all our observations at the VBT used thinned, back-illuminated, 1024 × 1024 pixel format CCD chips from Tektronics Inc., USA. We list in Table 2 the parameters of the chips we have employed.

Table 2. CCD parameters

Properties	CCD#1	CCD#2	CCD#3
Period	1995Sep–1997Apr	1997May–1999Mar 2000Feb–Mar	1999Apr–2000Apr
Size of array (pixel^2)	1024×1024	1024×1024	1024×1024
Image Scale (arcsec pixel^{-1})	0.609	0.604	0.608
Quantum Efficiency (at 550nm)	60%	68%	70%
Gain (e^-/ADU)	5.9	8.9	4.5
Read Noise (e^-)	8.0	9.8	9.1

For imaging faint sources, only integration times longer than a few hours can ensure sufficient signal-to-noise ratios. However, there are low-level systematics that set limits to the longest integration times and thus the accuracy of the photometry: variations due to the weather (night sky, cloud drifts), etc. A way to circumvent this problem is to make good use of the highest efficiency, linear, stable CCD detector and configure the image acquisition and processing techniques to cancel the systematics. We have used the shift-and-stare technique that is especially useful for fields containing faint objects that are much smaller than the angular size of the CCD. The procedure consists of taking several (even several tens of) short (but sky-limited), well-guided exposures of the field, with successive exposures randomly offset with respect to each other. There must be sufficient overlap (say 80%) of the successive fields as well as a minimum offset that is larger than the angular size of the largest bright object in the image. The final size of the image is

the common overlap area of all the frames. This set of unaligned images contains all the information about the celestial objects as well as the CCD systematics in extricable form. Then, registering the flat-fielded frames and median combining them within each filter subset leads to final images that are more or less limited by sky (Poisson) noise. Residual noise in the background is ameliorated due to the smoothing of the CCD response on several pixels for the same point on the celestial object.

Prior to 1997, we acquired long (about 45min) single exposures of the clusters instead of using the shift-and-stare. Subsequently, during each observing run we acquired multiple (at least three per filter), sky-limited exposures (typical exposure time ~10min) of the clusters of galaxies, short exposures (about 1 min) of standard stars for photometric calibration, and several CCD bias frames and twilight sky flat-fields for calibration of CCD systematics. Since the CCD detector is well-cooled making dark current negligible, we did not spend time on acquiring dark frames. We scheduled the cluster observations so that the objects were always at small zenith angles, to minimize atmospheric extinction. We chose the open cluster M67 and several Standard Area stars from Landolt (1992) for photometric transformation into the standard system and nightly zero-point calibrations.

The seeing (measured as the full width at half-maximum (FWHM) of an unresolved source in a well-focused and tracked image) is typically 1.5–2.5 arcsec. For the sky exposures in all the runs, we found that the corners of images were corrupted by vignetting from optics plus under-sized filters. The vignetting affects 10–12% of the CCD area, and varies slightly depending on the object position in the sky.

3. CCD Data Reduction

We used the Image Reduction and Analysis Facility (IRAF)[1] for reduction of CCD data and photometry, and the Faint Object Classification and Analysis System (FOCAS; Jarvis and Tyson 1981, Valdes 1982) for automatic detection, cataloging, and classification of objects as stars or galaxies.

Our CCD data processing consisted of the following sequence:

1. extrication of the instrumental signatures of the detector, filters and telescope by bias-subtraction, followed by flat-fielding
2. cosmic-ray cleaning and repair of bad pixels
3. registration of the multiple images of an individual cluster to a common co-ordinate system using astrometric information, and

[1] IRAF is distributed by the National Optical Astronomy Observatories, which are operated by the Association of Universities for Research in Astronomy, Inc., under cooperative agreement with the National Science Foundation.

4. co-addition of these registered frames into deep images.

We shall elaborate on each of these in the following sections.

3.1 CCD Data Pre-Processing

We performed the same preprocessing on both the science and standard star images. For bias-subtraction, we combined typically 6–8 zero exposure bias frames per night, to reduce the variations due to read-noise. For the CCDs used except during the 1999 April and 2000 February runs, we found that the bias images showed no gradient or any other non-uniformities. So, for these data sets, we bias-subtracted all frames using the median value of the bias-frame pixels (excluding the 10 edge rows and columns) as the bias value over each night. For the 1999 April and the 2000 February observations, where the bias frames showed repeatable systematic patterns of the order of a few counts, we have subtracted the combined nightly bias frames themselves from all the other exposures.

To account for the CCD pixel-to-pixel sensitivity variations, we created master flat-field frames by median-combining the twilight flat-field frames in each filter. Prior to combining them, we scaled the individual frames by the mode of their pixel values to take into account the differences in signal-to-noise ratios. We found that the combined frames were clear of stars but retained the vignetting pattern. We normalized these flats by the mean of the values in the unvignetted area of the frames. We flat-fielded every bias-subtracted object frame using the master flat in the corresponding filter. Flat-fielding successfully removed the vignetting pattern to a large extent. The processed science frames were fairly uniform, with residual sky-background inhomogenieties of $< 0.5\%$ over the full extent of each frame.

All the CCDs we used showed very few cosmetic defects such as bad or hot pixels. We fixed the bad columns that are due to faulty registers by linear interpolation across the columns. We did not otherwise repair bad pixels or create bad pixel masks. Since we had planned our shift-and-stare observations so that such defects do not affect the observed objects, we would not be hampered by ignoring this step. Finally, the object detector and classifier routines (discussed below) are capable of discriminating against "noise" including bad pixel rows or columns, cosmic ray events, etc.

We normally see about 10 cosmic ray events per minute registered on the CCD, and limited in size to 2–3 pixels. Where multiple exposures of the same object were available, we used the median filtering algorithm to reject these deviant measurements. In the cases where only single images were available (and while performing standard star photometry) we used tasks within IRAF to clean cosmic rays.

3.2 Astrometry and Image Registration

We observed the poor clusters over a period of 4-5 years. For a given cluster, the galaxies in the different exposures will not be recorded on the same pixel because of the shift-and-stare technique of observation as well as due to the small changes in the CCD Dewar orientation. So, the stack of such shifted images ought to be aligned before being combined into deeper images with better signal-to-noise ratios. We registered the images for a given cluster field by identifying approximately 20 unsaturated stars (detectable in all four passbands and over a majority of the different nights) to be used as astrometric reference points. To improve the accuracy with which centroids of the stars can be computed, we first magnified all the images by a factor of two in both the x and y axes using a bicubic natural spline interpolator. We used the flux conserving option in the magnification process, since we are interested in performing photometry on the resulting registered images. As the stellar profiles are well sampled, there is no degradation of the image during the interpolation to the larger image.

We needed to relate positions of the stars on the CCD images to their positions on the sky, and set the relationship between pixel coordinates and sky coordinates, i.e., the world coordinate system in the image headers. For the unsaturated stars, we identified the celestial co-ordinates (right ascension and declination in J2000 equinox) from the US Naval Observatory's Precision Measuring Machine (PMM) Project database. The PMM positions have relative accuracies of 0.1 arcsec. We derived the centroids of the reference stars, then matched their celestial and pixel coordinates. Using these, we computed the absolute astrometric solutions and updated the world coordinate system (WCS) header information for all the images.

Next we created an artificial image whose dimensions were roughly as large as the combined area covered by all the cluster images, and assigned it a WCS centered on the brightest cluster galaxy optical position. We then computed the mean x- and y-offsets and rotation of the reference stars of every frame relative to their locations in the fiducial image and averaged these to define the final values. Next, we geometrically re-mapped all image data for the cluster to match the fiducial coordinate system using a flux-conserving Lagrangian interpolation scheme to achieve registration at the subpixel level. Typical alignment accuracies in our equatorial coordinates are about 0.3 arcsec and at worst 0.6 arcsec. These compare favorably with the CCD pixel scale of 0.61 arcsec and seeing of 1.5–2.5 arcsec. Once we registered all frames of a given cluster to a common coordinate system, we co-added the best independent exposures in each passband to produce four "deep" *BVRI* images. Generally, we made an effort to combine images only if the signal-to-noise ratios were similar, the seeing was better than 2.5 arcsec, and if the number of common objects was at least 50%. Prior to combining, we scaled the individual images such that several of the stars common to them had the same counts within one FWHM. During the combining operation, we weighted the images by their exposure time. We further co-added these deep images to create an enlarged mosaic image of each cluster. To restore the magnified co-added images to their original scale,

we then block summed them over two columns and lines. These final images served as the master frames that we would use for object detection through FOCAS. The mosaics improved upon the areal coverage of the single CCD field of view by about 2 arcmin for each cluster.

4. Construction of Galaxy Catalogs

In this section, we describe the detection of faint objects in the cluster frames and their subsequent classification as stars or galaxies employing the FOCAS package. We then explain the optical photometry and the characteristics of the final catalogs of galaxies in the fields of the four poor clusters.

4.1 Object Detection and Preliminary Cataloging

FOCAS assembles a catalog of faint objects in an image by searching for a minimum number of contiguous pixels that are some sigma above the local sky background which it first determines from the image. FOCAS requires input of three parameters that can be configured for optimal detection. We tuned these parameters in the following manner:

1. pixel detection threshold sigma = 4.5–5× the local sky noise
2. minimum pixel area or object size = $0.9\times(\mathrm{FWHM})^2$
3. spatial convolving filter = the FOCAS "built-in" filter

As we were working with co-added *BVRI* images (composed of unequal numbers of individual frames of various filters), we had to first experiment with a range of thresholds — in combination with the other two search parameters — for robust object detection. Lowering the detection threshold includes low surface brightness objects but at the cost of rising contamination by spurious objects, most of which will be the faintest in the catalog.

Our choice of the minimum number of object pixels was directed by the expected size of the cluster galaxies and the image seeing. A canonical galaxy size of 10 kpc projects angular diameters of about 7 arcsec and 3 arcsec for redshifts z=0.075 and z=0.25 respectively (for $H_0 = 100$). Our image seeing was at best 1.5 arcsec in the mosaicked images; galaxies smaller than 10 kpc would be practically point-like. So, rather than fix an arbitrary constant detection area, we opted to fix the minimum object size to 0.8 times the area within the half-light radius of the image point spread function (PSF). For a 2-D Gaussian PSF, this translates to $0.9\times(\mathrm{FWHM})^2$; in our images this minimum area is typically $\approx$ 15 pixels.

To assist in the revealing of very faint objects which may be only a few percent of the sky intensity, FOCAS convolves the image with a 2-D weighting function called the detection filter. If this spatial convolution filter has a profile similar to the object, then it maximizes the signal-to-noise ratio of the object detection. Obviously it is not possible to determine *à priori* the profiles of the galaxies to be detected! On account of this and the expectation that a large number of galaxies will be barely resolved in our images, we have opted for the FOCAS "built-in" filter, a diagonally symmetric filter.

With the parameters listed above, we first ran the object detector on each of the four deep cluster images to produce catalogs that contain (pixel) positional information, (uncalibrated) magnitudes, radial moments and shape parameters such as ellipticity and position angle of the objects. Subsequently, we ran FOCAS to split objects that showed merged isophotes: each of the multiple components must satisfy the minimum area criterion to be declared a new object. FOCAS automatically updates the catalogs to include the split objects.

The detector runs into trouble near very bright stars where it detects many spurious objects in the spilled light halos, and in picking out the tenuous extended halos of the brightest cluster members. We therefore reviewed the created catalogs by eye to verify the authenticity of objects. Typically, between 3 and 5% of the small, dim objects turned out to be contaminants. Of course, manual removal of suspected objects in stellar halos may have the unwelcome side-effect of deleting real, faint objects; however, the number of such interventions is very small and is negligible at magnitudes where the catalogs are complete.

4.2 Star–Galaxy Discrimination

Though we detect objects in only one combined image per cluster, we measure their structural and photometric properties and classify them on the multiple images combined *separately* in each passband. We bifurcated the detected objects into stellar and extended objects using the built-in FOCAS classifier that is based on the resolution classifier algorithm described in Valdes (1982b). First, we determined the PSF in each image from a manually selected set of isolated, unsaturated stars many of which had served in the astrometry as well. To assure ourselves that the PSF is not inappropriate, we inspected the PSF visually and compared it quickly with the compact, symmetric objects on the image. From this PSF, FOCAS creates a general template that is basically a scaled PSF with a second component that could be narrower or broader. FOCAS classifies objects into "stars", "galaxies", or "noise" depending on how well they are fit by the scaled nominal PSF and the extended component.

After running the classifier on the various filter images available for each cluster, we assigned one of the above classes if FOCAS had classified it in the same way in at least 50% of the images or in at least two different filters. Therefore, the assignment of the

class is unlikely to be dominated by the color of the object. We manually edited the final catalog to put in the final object classification. Having multiple images to create several independent classifications makes the exercise rather secure. We further performed visual checks of the automated object classification to ensure its validity. While visual inspection is definitely laborious and itself not entirely error-free, it is nonetheless a valuable step in faint object analysis.

4.3 Photometry and Photometric Calibration

On completion of the above analyses, the result is a catalog of positions, pixel areas, crude photometry, etc. of objects classified into stars and galaxies. Valdes (1982), the author of FOCAS, cautions against using the software for accurate photometry. We therefore performed aperture photometry of all objects (whose CCD pixel positions were derived by FOCAS) with the IRAF PHOT task.

We started by applying a centroiding algorithm to determine the position of the aperture center more accurately. We used a 3 arcsec radius circular aperture for the photometry, and a sky annulus ~ 5 arcsec wide and ~ 9 arcsec away. The 3 arcsec aperture was the best compromise between enclosing all the light from the object and minimizing errors due to varying focus, seeing or sky. We then applied aperture corrections to correct the magnitudes measured within the 3 arcsec aperture to the 6.6 arcsec radius within which we computed the standard star magnitudes. We estimated the aperture corrections using nearly a dozen bright, isolated stars in the particular images.

We chose to transform our instrumental magnitudes to the standard Johnson-Morgan BV and Kron-Cousins R_cI_c broadband systems using the old Galactic cluster M67 for which many studies are available. We used standard stars from Selected Areas of Landolt (1992) for nightly zero-point calibrations of our observations. To determine the transformation co-efficients from our instrumental magnitudes to the standard system, we used the following equations:

$$\begin{aligned}
(B-V) &= \alpha_{(b-v)} + \beta_{(b-v)}(b-v) \\
(V-R) &\stackrel{\pi}{=} \alpha_{(v-r)} + \beta_{(v-r)}(v-r) \\
(R-I) &= \alpha_{(r-i)} + \beta_{(r-i)}(r-i) \\
(V-v) &= \alpha_{bv} + \beta_{bv}(B-V)_i \\
&= \alpha_{vr} + \beta_{vr}(V-R)_i
\end{aligned}$$

where the capital letters denote magnitudes on the standard system, the small letters instrumental magnitudes and the subscripts "i" denote our "standardised" color indices.

In Table 5 we list the coefficients α and β and their standard deviations derived from linear Chi-squares fits to the M67 data over the observing period. The fiducial zeropoint we have used in transforming CCD counts into magnitudes is 25.0 mag. We see that

the formal errors associated with the photometric transformation parameters are a few percent at most. At $V = 20$ mag, we find that the total uncertainty in photometric calibration is about 0.07 mag. We made an independent check of the reliability of our photometry by matching our stellar locus with values for stellar colors from the literature. The match was not exact, but the systematic errors were within about 5%.

4.4 Galactic Extinction Correction

We used the values from the NASA/IPAC Extragalactic Database (NED) based on B-band extinctions derived by Schlegel et al. (1998) and converted to other bands assuming $R_V = 3.1$ according to the prescriptions in Cardelli et al. (1989). We list the computed extinction corrections in Table 3.

Though the cluster MS0301 is at high Galactic latitude ($|b| > 35°$), the extinction towards it is anomalously high due to a "spur" of Galactic clouds along this longitude. The canonical value of $R_V = 3.1$ is probably not valid for this region, but lacking independent estimation of R_V, we continue to use it. For the other three clusters, the extinction correction is about $1.5 - 2$ times the photometric errors at $V = 20$ mag.

Table 3. Galactic extinction corrections in magnitudes, in the four bands towards the EMSS poor clusters studied in this work.

EMSS Cluster	b	A_B	A_V	A_R	A_I
MS 0002.8+1556	−45.23	–	0.16	0.13	–
MS 0301.7+1516	−36.56	0.72	0.55	0.45	0.33
MS 0735.6+7421	+29.44	0.10	0.08	0.06	0.04
MS 1306.7−0121	+60.93	0.12	0.09	0.08	0.06

4.5 Catalog Completeness and Misclassification

We constructed the final catalog of faint objects with those that could be detected and photometered in at least two individual images among the four different filters. We present the catalogs of galaxies in MS 0002.8+1556 in Table 6, MS 0301.7+1516 in Table 7, MS 0735.6+7421 in Table 8, and MS 1306.7−0121 in Table 9. Note that these include all extended objects in the CCD field of view; at this stage, we do not know which of them belong to the clusters or are fore- or back-ground objects.

We now need to estimate the object detection efficiency of FOCAS (i.e., the percent of all objects in an image that FOCAS catalogs), and understand how reliably FOCAS

classifies objects (or how often stellar objects are misclassified as nonstellar and vice versa). In the literature, there are different methods of determining the completeness of detection and reliability of classification of faint objects. These include (i) addition of accurately simulated objects of known range of magnitude and morphology to the observed images, and (ii) creation of artificial data matching the real data. One processes these images in a manner similar to the original images, produces the catalog of objects, and then compares the output catalog with the input catalogs of the artificial stars and galaxies. It is then straightforward to estimate the completeness and classification reliability of the software. However, the slightly varying PSF among many of our CCD frames makes it difficult to accurately add similar artificial objects. Similarly, it is not straightforward to use entirely artificial data, since their parameters may not be matched exactly with our real data. A third strategy is to use the differential luminosity function of galaxies. Now, field galaxy counts in the literature (e.g., Tyson 1988) show a monotonic increase (with steeper slopes in bluer bands) and appear to saturate at only $\approx B = 27$ mag. Therefore, a maximum in the histogram *before* such photometric depth implies the onset of statistical incompleteness in our sample.

We plot the differential luminosity function, i.e., the frequency distribution of the galaxy number counts within apparent magnitude bins of 0.2 mag, in Fig. 1. The relative number of objects rises linearly until a turnover occurs around $21 < V < 22$. We take the completeness limit (small arrows in the figures) of our data conservatively at 0.2 mag brighter than the peak of each histogram. These set the depth of our galaxy samples for the further analysis (construction of cluster galaxy luminosity functions, color-magnitude relations, etc.) are reported in a separate paper (Sharma & Prabhu 2002).

Here we must bear in mind that object detection depends on seeing — if poor seeing blurs an extended object, its very faint outer isophotes would fall below the surface brightness threshold cutoff, rendering the object fainter and smaller, thus more difficult to detect (and more prone to misclassification as a star). We have attempted to avoid this problem by using only those images where the stellar profiles have full-width-at-half-maximum of < 2 arcsec (see also below). Crowding of objects is another pitfall; however, our poor clusters are not crowded fields (by their very nature). They are also at high Galactic latitude where stellar densities are not large. Therefore, crowding hardly contributes to uncertainties in completeness.

The assignment of stellar/non-stellar class to a detected object was on the basis of its receiving the same classification in at least 50% of the images in the different filters. The internal accuracy of the classifier — tested by comparing object classification in the multiple images — is rather dependent on the faintness of the object and on image seeing. Poor seeing will of course degrade the smaller extended objects into unresolved sources. As Fig. 2 shows, in a plot of the logarithm of object area against the (extinction-corrected) V magnitude, stars and extended objects occupy two separate loci. Clearly, and expectedly, the apparent areas (radii) of bright galaxies are systematically larger than those of stars at the same apparent magnitude, while faint galaxies merge with

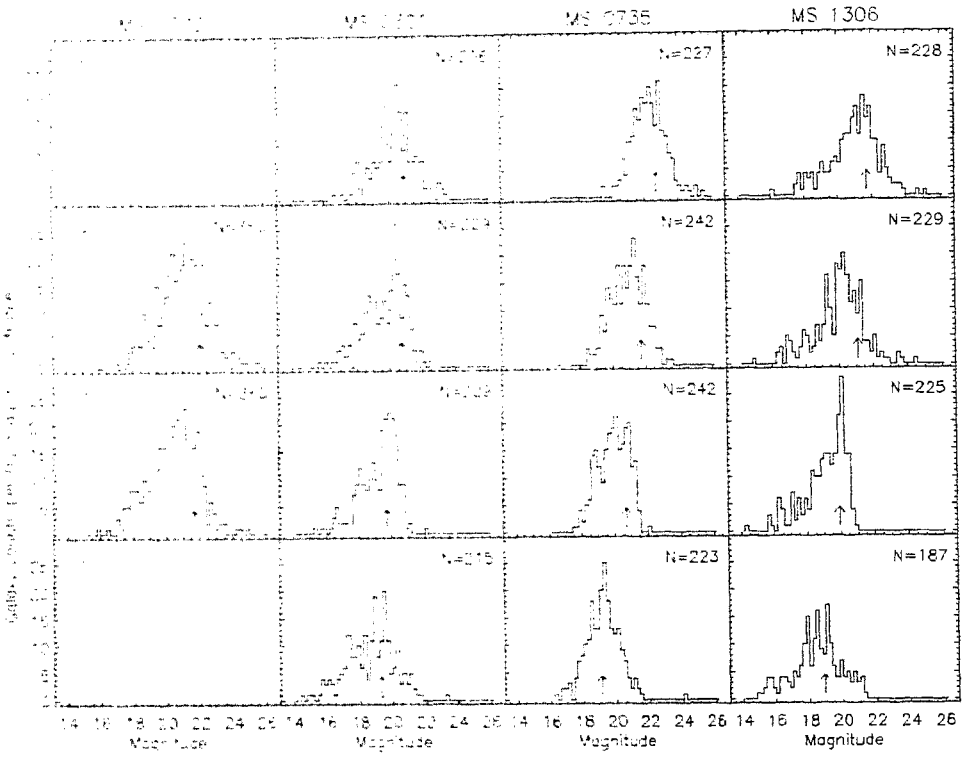

Figure 1. Galaxy counts in the CCD frames centered on the BCMs. Small vertical arrows denote the limit of completeness.

stars. In fact, for seeing greater than the typical scale sizes of the objects, it is possible that objects of differing magnitudes would be smoothed to a similar size comparable to the seeing disk. The threshold of discrimination, which therefore depends crucially on the observed size of the objects, is roughly $V = 19.5$ after which the distinction is blurred. This magnitude expectedly corresponds to an object area of radius about the ≈ 2 arcsec seeing disk. A smaller stellar FWHM would have made the stellar envelop narrower and improved the bifurcation limits to fainter magnitudes.

In fact, FOCAS uses several parameters for bifurcation of objects (more than merely the locus in the area vs. magnitude) simultaneously (Valdes 1982b), so Fig. 2 is merely an indication of the trend of the reliability of the classifier and is most likely an underestimate. For the brightest objects ($14 < m_V < 17$), there is virtual unanimity in the FOCAS classifications in the images in different filters. At $V \approx 20$ mag ($R \approx 19$ mag), where the surface number density of stars and galaxies are comparable, the fraction of objects that received conflicting classifications is $\sim 10\%$; this rises disappointingly to

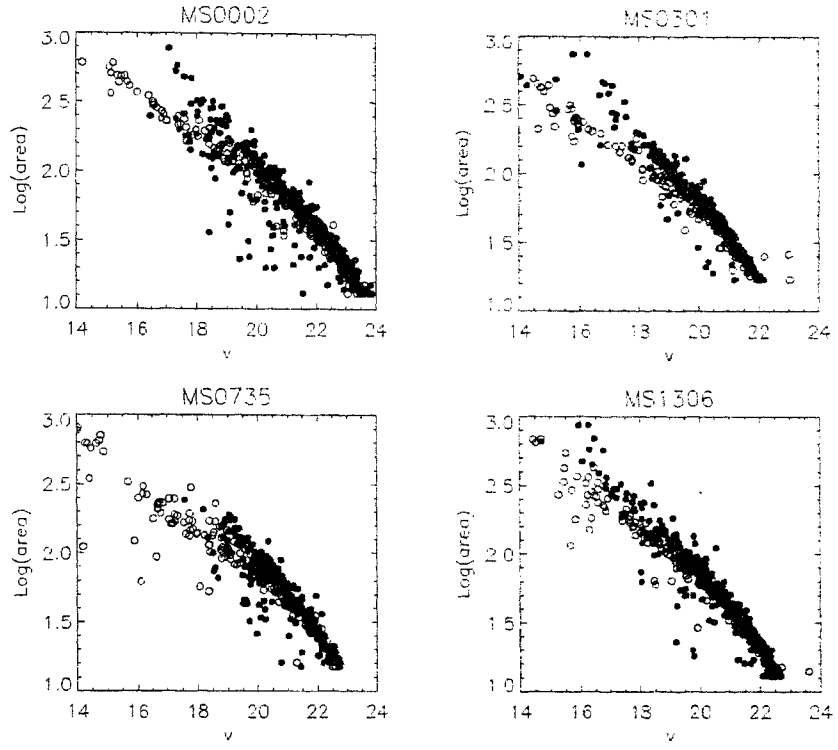

Figure 2. Star–galaxy separation plots for the EMSS poor cluster images. Stellar (open circles) and non-stellar objects (filled circles) occupy separate regions in the plot of logarithm of area vs. m_V, with stars having higher surface brightness than extended objects.

$\sim$ 30% about 3 magnitudes fainter. Sometimes, FOCAS classified closely paired objects as galaxies; visual inspection usually clarified such discrepancies. In particular, visual inspection and object colors show that some 10% of galaxies fainter than 21.5 mag (close to the completeness limit) could be misclassified as stellar objects, while some stellar objects could well be QSOs. Adding the relevant contributions due to misclassification to the galaxy counts changes the overall faint number counts non-negligibly but without seriously improving the completeness levels. In fact, due to the relatively shallow number counts of stars (e.g., Bahcall & Soneira 1981) versus galaxies (e.g., Tyson 1988), the fractional stellar contamination actually decreases with increasing magnitude as shown in Fig. 3.

We conclude that our detection algorithm and photometry are complete to about $V = 21$ mag within errors of $< 10\%$, and our star–galaxy separation does not significantly contaminate the galaxy catalogs with stellar objects.

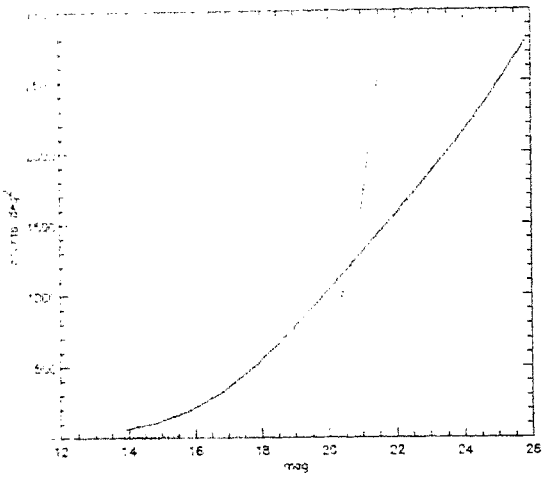

Figure 3. Number counts of stars and galaxies in the direction of MS1306. The solid line is the prediction of the Bahcall & Soneira (1981) model of Galactic star counts, and the dotted line is the empirical 'field galaxy' count of Wilson et al. (1997), both in the V band. Notice that by $V \approx 20$ mag, galaxies begin to dominate over stars.

5. Discussion and Conclusions

We construct our sample of moderate-redshift ($0.08 < z < 0.25$) poor clusters from the X-ray selected EMSS cluster catalog of Gioia & Luppino (1994; GL94). These objects have X-ray luminosities $L_X \geq 3 \times 10^{43} \mathrm{erg\,s^{-1}}$, have their X-ray centroid optically identified with galaxy over-densities and are noted by GL94 as being optically poor. We acquired optical CCD images of four poor clusters, and after pre-processing the data, detected the faint objects in the fields and separated them into stars and extended objects. We performed aperture photometry (corrected to ≈ 7 arcsec) transformed to the standard Johnson–Cousins' B, V, R and I bandpasses. The galaxy catalogs are complete to about $V = 21$ mag, or $\approx M_V = -18$ in the rest-frame of the different clusters. We now proceed to measure the sizes and richness of the four clusters.

To estimate the expanse of the clusters, we have to deal with their central density contrast being only a few times that of the field. Rather than construct an azimuthally-averaged profile of the surface distribution of the galaxies as is the norm in the literature, we use a procedure proposed by Yamagata & Maehara (1986) for MKW/AWM poor clusters. This consists of determining the maximum radius where the cumulative galaxy count (to different magnitude limits) shows an appreciable excess over the field value. We use the R-band magnitudes for our cluster catalogs and plot the resulting curves in Fig. 4. From this, we conclude that the poor clusters extend to about 4 arcmin with MS1306

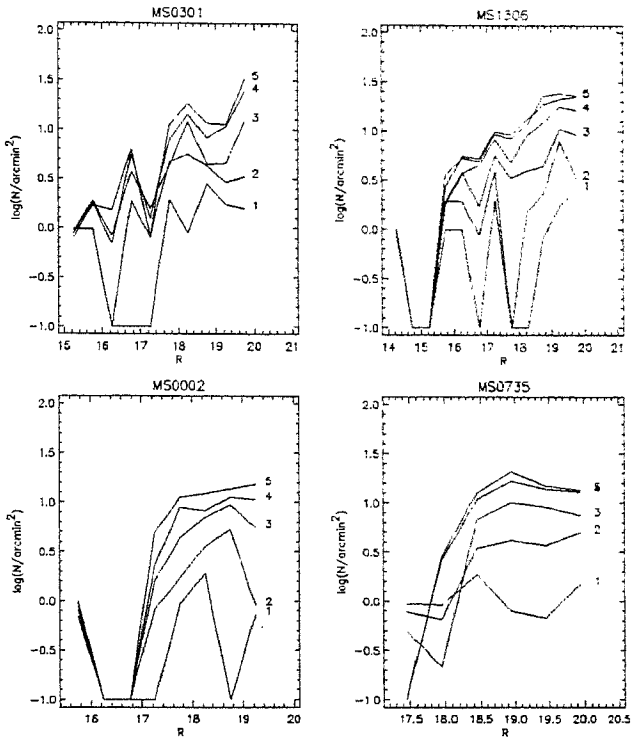

Figure 4. Radial extent of the poor clusters.

(of size > 5arcmin) being the most extended. The corresponding metric sizes are about 500 kpc for MS0301 and MS1306, 650 kpc for MS0002 and about 1.0 Mpc for MS0735. The cluster galaxy densities within the central 3-4 arcminutes are significantly higher than that expected from the field counts. Indeed, the sizes we determine for MS1306 and MS0002 are quite consistent with their diffuse X-ray extents determined in the Einstein Extended Sources Survey (Oppenheimer et al. 1997).

A 0.5 Mpc radius corresponds to the typical size of the X-ray emitting region for poor clusters (e.g., Doe et al. 1995). It is also a good metric size within which to estimate the richness of poor clusters, as it permits a compromise between the competing demands of good signal in cluster counts and minimizing the background uncertainty. Among the richness estimates in the literature, two that are apt for poor clusters are:

1. the Bahcall (1977) richness parameter $N_{0.5}$: the average surface density of galaxies brighter than $m_3 + 2$ within the innermost circle of radius 0.5 Mpc around the cluster center after correction for the background, and
2. the Allington-Smith et al. (1993) richness estimate $N_{0.5}^{-19}$: the membership of the

cluster to a fixed absolute magnitude limit of $M_V = -19$ within the same 0.5 Mpc radius, corrected for the background.

Table 4 provides the two richness estimates in V band for our poor clusters. We calculate these using all galaxies within the required metric areas after identifying the brightest cluster galaxy with the cluster center. We correct for the background using the field galaxy counts of Wilson et al. (1997). The formal errors are 1σ estimates assuming Poisson statistics which, realistically speaking, underestimate the true errors due to the clustering of galaxies. Potential errors with misidentification of the third most luminous member could result in not sampling the same region of the LF and thus affect the $N_{0.5}$ estimate; this is not a concern, however, for the $N_{0.5}^{-19}$ richness estimate.

Table 4. Cluster richness estimates. Column 2 - $N_{0.5}$ of Bahcall (1977), Col. 3 - $N_{0.5}^{-19}$ of Allington-Smith et al. (1993), Col. 4 - V absolute magnitude of the third brightest cluster galaxy.

Cluster	$N_{0.5}$	$N_{0.5}^{-19}$	M_3
MS0002	30±6	31±7	-21.04
MS0301	31±6	42±8	-21.51
MS0735	21±5	22±6	-21.25
MS1306	19±5	33±7	-22.06

Our clusters have a richness parameter twice that of Virgo ($N_0 = 11$; Bahcall 1977) and about four times that for the poor groups of Allington-Smith et al. (1993) whose mean $N_{0.5}^{-19} = 7.2 \pm 1.0$, with $-6.7 \pm 5.6 \leq N_{0.5}^{-19} \leq 31.6 \pm 7.4$. Note that the conversion between angular to metric sizes depends on the assumed values of H_0 and (with small effect for our redshift range) q_0. We use the same value of H_0 as both Bahcall (1977) and Allington-Smith et al. (1993); however, we use $q_0 = 0.5$. Had we used $q_0 = 0.0$, the angular radius corresponding to 0.5 Mpc would decrease by about 5% at $z = 0.22$, decreasing the richness estimate by a few percent if $N \propto r$ as may be true for rich clusters. Since our error estimates are inevitably larger than a few percent, we do not worry about the effect of cosmological parameters in a comparison of richness class.

In separate papers, we shall study the detailed statistical properties of the galaxies in the poor clusters, as well as the structure of their brightest members. It would be of interest to undertake multi-object spectroscopy to characterize the poor clusters better in terms of membership, to determine their velocity dispersion, and to map their internal dynamics. Imaging that is deeper and of higher spatial resolution is necessary to determine the morphologies of member galaxies, and to ascertain if the systems contain intracluster light presumably contributed by tidal debris.

Acknowledgments

This work has been carried out using the observing and computing facilities of the Indian Institute of Astrophysics, Bangalore. We thank the Vainu Bappu Observatory Time Allocation Committee for allotting — season after season — dark nights for our observing program. The observing assistants and technical support staff of the VBT gave us generous, competent assistance during the clear runs as well as commiseration on the clouded nights. This research has made use of the NASA/IPAC Extra-galactic Database (NED) which is operated by the Jet Propulsion Laboratory, Caltech, under contract with the National Aeronautics and Space Administration. It has also made use of NASA's Astrophysics Data System Bibliographic Services, the USNOFS Image and Catalogue Archive operated by the United States Naval Observatory, Flagstaff Station, and the APS Catalog of POSS I which is supported by the National Aeronautics and Space Administration and and the University of Minnesota.

References

Abell, G. O. 1958, Ap.J.Supp.Series, 3, 211
Allington-Smith, J.R., Ellis, R., Zirbel, E.L., & Oemler, A., Jr. 1993, Ap.J., 404, 521
Bahcall N. A. 1977, Ap.J.Lett., 217, L77
Bahcall N. A. 1980, Ap.J.Lett., 238, L117
Bahcall, J. N. & Soneira, R. M. 1981, Ap.J.Supp.Series, 47, 357
Beers, T.C., Kriessler, J.R., Bird, C.M., & Huchra, J.P. 1995, A.J., 109, 874
Briel, U. G. & Henry, J. P. 1993, A.&A., 278, 37
Burns, J.O., et al., 1996, Ap.J., 467, L49
Caldwell, N. & Rose, J. 1997, A.J., 113, 492
Cardelli, J.A., Clayton, G.C., & Mathis, J.S. 1989, Ap.J., 345, 245
Doe, S.M., Ledlow, M.J., Burns, J.O., & White, R.A. 1995, A.J., 110, 46
Dressler, A. 1984, A.R.A.&A., 22, 185
Fukugita, M., Shimasaku, K., & Ichikawa, T. 1995, P.A.S.P., 107, 945
Gioia, I. M., Henry, J. P., Maccacaro, T., Morris, S. L., Stocke, J. T., & Wolter, A. 1990, Ap.J.Lett., 356, L35
Gioia, I. M. & Luppino, G. A. 1994, Ap.J.Supp.Series, 94, 583
Giuricin, G., Marinoni, C., Ceriani, L., & Pisani, A. 2000, Ap.J., 543, 178
Hickson, P. 1997, A.R.A.&A., 35, 357
Jarvis, J. F. & Tyson, J. A. 1981, A.J., 86, 476
Landolt A. 1992, A.J., 104, 340
Ledlow, M. J., Loken, C., Burns, J. O., Hill, J. M., & White, R. A., 1996, A.J., 112, 388
Mahdavi, A., Böhringer, H., Geller, M. J., & Ramella, M., 2000, Ap.J., 534, 114
Mulchaey, J. S. 2000, A.R.A.&A., 38, 289
Oppenheimer, B. R., Helfand, D. J., & Gaidos, E. J. 1997, A.J., 113, 2134
Pennington, R. L., et al., 1993, P.A.S.P., 105, 521
Ponman, T., Bourner, P., Ebeling, H., & Bohringer, H. 1996, M.N.R.A.S, 283, 690
Rector, T. A., Stocke, J. T., & Perlman, E. S. 1999, Ap.J., 516, 145
Scharf, C.A., Jones, L.R.L., Ebeling, H., Perlman, E., Malkam , M., & Wegner, G. 1997, Ap.J., 477, 79

Schlegel, D.J., Finkbeiner, D.P., & Davis, M. 1998, Ap.J., 500, 525
Sharma, M., & Prabhu, T. P., 2002, in preparation
Tyson, J. A. 1988, A.J., 96, 1
Valdes, F. 1982a, FOCAS User's Manual, Kitt Peak National Observatory, Central Computer Services, Tucson, AZ, USA
Valdes, F. 1982b, The Resolution Classifier, in Instrumentation in Astronomy IV, SPIE Proceedings, 331, 465
Vikhlinin, A., et al., 1998, Ap.J., 502, 558
White, R. A., et al., 1999, A.J., 118, 2014
Wilson, G., Smail, I., Ellis, R. S., & Couch, W. J. 1997, M.N.R.A.S, 284, 915
Yamagata, T. & Maehara, H. 1986, Astrophysics and Space Science, 118, 459

Table 5. The journal of cluster observations. The table shows the cluster name, filter, date, exposure time in seconds, and airmass.

Object	Filter	Date	Exposure	Airmass
MS0002	V	1997 Oct 05	600	1.24
			600	1.18
			600	1.14
			720	1.11
			600	1.05
			600	1.04
	R	1997 Oct 05	600	1.04
			600	1.06
			600	1.08
MS0301	B	1995 Dec 19	2700	1.05
		2000 Feb 01	1800	1.07
	V	1997 Oct 05	600	1.01
		1998 Jan 22	600	1.04
			600	1.06
			600	1.08
		1998 Dec 21	600	1.11
			600	1.03
			600	1.04
			600	1.08
			600	1.11
			600	1.03
	R	1995 Dec 19	1800	1.02
		1997 Oct 05	600	1.01
			600	1.02
			600	1.03
		1998 Jan 22	600	1.00
			600	1.01
			600	1.02
	I	1995 Dec 19	1800	1.06
MS0735	B	2000 Jan 08	720	2.15
			720	2.13
			900	2.12
			900	2.11
			900	2.11
	V	1997 Mar 07	1200	2.13
			1200	2.18
			1500	2.24
	R	1997 Mar 07	1200	2.34
		1997 Mar 08	1200	2.11
			1200	2.11
			1200	2.12
	I	1997 Mar 08	1200	2.16
			1200	2.21
			1200	2.27
MS1306	B	1996 Feb 16	2700	1.04
	V	1996 Feb 16	2700	1.04
	R	1996 Feb 16	900	1.03
		1996 Feb 17	1800	1.03
		1996 Apr 22	1200	1.13
			900	1.22
		1997 Apr 07	900	1.04
			900	1.05
		2000 Mar 05	900	1.20
	I	1996 Feb 17	1800	1.04

Table 6. Coefficients of the photometric transformation equations 1.

[illegible]	[illegible]	Index	a	stddev$_a$	b	stddev$_b$
[illegible]	[illegible]	$(B-V)$	0.821	0.003	1.161	0.015
March 11	Filters#1	$(V-I_c)$	0.856	0.002	1.011	0.004
		$V_{(B-V)}$	-0.310	0.008	0.020	0.011
		$V_{(V-I_c)}$	-0.313	0.008	0.022	0.011
[illegible]	[illegible]	$(B-V)$	-1.552	0.008	1.439	0.025
April 22	Filters#1	$(V-R_c)$	-0.122	0.006	0.996	0.015
		$V_{(B-V)}$	-1.589	0.009	0.024	0.014
		$V_{(V-R)}$	-1.592	0.010	0.048	0.028
1996	CCD#1	$(B-V)$			1.439	0.025
AVERAGE	Filters#1	$V_{(B-V)}$			0.022	0.011
1997	CCD#2	$(B-V)$	-1.252	0.022	0.988	0.011
March 07	Filters#2	$(V-R_c)$	-0.252	0.011	0.950	0.017
		$(V-I_c)$	-0.104	0.032	0.973	0.038
		$V_{(B-V)}$	-4.059	0.017	0.059	0.026
		$V_{(V-R)}$	-4.083	0.027	0.162	0.073
[illegible]	CCD#2	$(B-V)$	-1.135	0.023	1.052	0.012
March 08	Filters#2	$(V-R_c)$	-0.335	0.010	1.000	0.014
		(R_c-I_c)	0.134	0.005	1.003	0.016
		$(V-I_c)$	-0.223	0.013	1.025	0.013
		$V_{(B-V)}$	-4.047	0.028	0.015	0.030
		$V_{(V-R)}$	-4.062	0.015	0.032	0.015
1997	CCD#2	$(B-V)$			1.020	0.012
AVERAGE	Filters#2	$(V-R_c)$			0.975	0.016
		$(V-I_c)$			1.000	0.020
		$V_{(B-V)}$			0.037	0.030
		$V_{(V-R)}$			0.097	0.070
1997	CCD#2	$(B-V)$	-1.268	0.007	0.976	0.004
April 06	Filters#3	$(V-R_c)$	-0.529	0.011	1.080	0.013
		$V_{(B-V)}$	-4.354	0.007	0.071	0.009
		$V_{(V-R)}$	-4.373	0.009	0.182	0.022
1998	CCD#2	$(B-V)$	-0.330	0.005	0.967	0.005
April 01	Filters#3	$(V-R_c)$	-0.960	0.022	1.081	0.019
		(R_c-I_c)	0.065	0.012	0.989	0.036
		$(V-I_c)$	-1.032	0.067	1.163	0.043
		$V_{(B-V)}$	-4.708	0.006	0.043	0.008
		$V_{(V-R)}$	-4.715	0.019	0.049	0.024
1999	CCD#3	$(B-V)$	-1.284	0.001	1.016	0.009
April 11	Filters#3	$(V-R_c)$	-0.351	0.001	1.022	0.006
		(R_c-I_c)	0.124	0.002	0.893	0.005
		$(V-I_c)$	-0.205	0.002	0.957	0.010
		$V_{(B-V)}$	-3.312	0.018	0.073	0.042
		$V_{(V-R)}$	-3.309	0.016	0.036	0.020
2000	CCD#2	$(B-V)$	-1.318	0.030	0.999	0.014
February 01	Filters#3	$(V-R_c)$	-0.514	0.016	1.045	0.017
		(R_c-I_c)	0.011	0.004	0.974	0.009
		$(V-I_c)$	-0.547	0.015	1.048	0.011
		$V_{(B-V)}$	-4.037	0.036	0.024	0.040
		$V_{(V-R)}$	-4.036	0.040	0.043	0.090
2000	CCD#2	$(B-V)$	-1.246	0.012	0.975	0.05
March 03	Filters#3	$(V-R_c)$	-0.531	0.017	1.043	0.012
		(R_c-I_c)	-0.030	0.008	0.951	0.011
		$(V-I_c)$	-0.620	0.019	1.060	0.014
		$V_{(B-V)}$	-4.140	0.009	0.086	0.010

Table 7. Catalog of galaxies in the field of MS 0002+1556.

R.A(2000)	Dec(2000)	V	B-V	V-R	R-I
0: 5: 2.6	16:14:58	19.51	–	0.43	–
0: 5: 2.9	16:15:24	21.67	–	-0.11	–
0: 5: 3.0	16:14:34	21.76	–	0.53	–
0: 5: 3.3	16: 9:41	21.75	–	0.68	–
0: 5: 3.3	16:13:24	21.59	–	0.93	–
0: 5: 3.3	16:17:17	21.37	–	0.08	–
0: 5: 3.4	16:14:42	20.14	–	0.56	–
0: 5: 3.4	16:14:50	18.73	–	0.56	–
0: 5: 3.7	16: 9:22	20.64	–	0.67	–
0: 5: 4.7	16:16:15	20.70	–	0.37	–
0: 5: 4.8	16:10:55	22.34	–	0.26	–
0: 5: 5.2	16: 9:26	22.66	–	0.54	–
0: 5: 5.2	16:15:29	21.51	–	0.46	–
0: 5: 5.4	16:10:58	22.28	–	1.59	–
0: 5: 5.6	16:12:25	19.62	–	0.84	–
0: 5: 5.7	16:10:42	19.38	–	0.62	–
0: 5: 5.7	16:11:23	22.95	–	1.04	–
0: 5: 5.7	16:11:42	22.65	–	0.74	–
0: 5: 5.7	16:15:55	21.53	–	0.39	–
0: 5: 6.0	16:16:40	20.25	–	0.43	–
0: 5: 6.2	16:10:44	22.85	–	1.48	–
0: 5: 6.2	16:14:25	21.59	–	0.87	–
0: 5: 6.2	16:15: 0	20.63	–	0.62	–
0: 5: 6.3	16: 9:10	21.89	–	0.39	–
0: 5: 6.6	16:11:35	24.16	–	1.04	–
0: 5: 6.6	16:12:20	21.24	–	1.13	–
0: 5: 6.6	16:15:42	20.25	–	0.41	–
0: 5: 7.2	16:15:42	20.82	–	0.40	–
0: 5: 7.4	16: 8:30	21.50	–	1.03	–
0: 5: 7.4	16:14:10	21.36	–	0.89	–
0: 5: 7.5	16:15:36	22.17	–	0.78	–
0: 5: 8.2	16:11:41	24.82	–	2.97	–
0: 5: 8.4	16:14: 9	21.87	–	1.07	–
0: 5: 8.5	16:11:55	24.46	–	2.84	–
0: 5: 8.5	16:12:33	18.61	–	0.68	–
0: 5: 8.7	16:14:30	20.08	–	0.64	–
0: 5: 8.7	16:15:43	22.45	–	0.87	–
0: 5: 8.7	16:16: 5	21.73	–	0.73	–
0: 5: 9.2	16: 8:41	19.26	–	0.54	–
0: 5: 9.7	16: 8:53	22.32	–	0.54	–
0: 5: 9.9	16: 8:58	23.29	–	1.30	–
0: 5: 9.9	16:11:18	21.87	–	0.94	–
0: 5: 9.9	16:16:57	20.52	–	0.44	–
0: 5:10.0	16: 9:13	19.11	–	0.59	–
0: 5:10.1	16: 8: 0	22.66	–	0.65	–
0: 5:10.1	16:13:35	23.11	–	1.72	–
0: 5:10.2	16: 8:33	28.01	–	–	–
0: 5:10.2	16:13:25	21.16	–	0.90	–
0: 5:10.2	16:16:53	21.63	–	0.65	–
0: 5:10.2	16:17:43	20.70	–	-0.30	–
0: 5:10.4	16:14:40	23.02	–	1.16	–
0: 5:10.5	16:13:48	21.79	–	1.26	–
0: 5:10.7	16:14: 3	22.24	–	0.92	–
0: 5:10.7	16:16:11	21.81	–	0.63	–
0: 5:10.8	16:10:36	19.84	–	0.61	–
0: 5:10.8	16:11:56	22.25	–	0.52	–
0: 5:10.9	16:17: 4	20.34	–	0.55	–
0: 5:11.1	16: 8:45	21.23	–	0.71	–
0: 5:11.1	16:17:21	21.20	–	0.21	–
0: 5:11.4	16:11:16	19.26	–	0.42	–
0: 5:11.6	16:16:30	20.40	–	0.31	–
0: 5:11.7	16: 8:40	21.39	–	0.66	–
0: 5:11.7	16:17: 8	21.21	–	0.40	–
0: 5:11.9	16:15:36	20.45	–	0.39	–
0: 5:12.4	16: 9:32	22.58	–	0.70	–
0: 5:12.6	16: 8: 3	22.23	–	-0.66	–

MS0002 contd.

R.A(2000)	Dec(2000)	V	B-V	V-R	R-I
0: 5:12.6	16:13:48	21.06	–	1.55	–
0: 5:12.7	16: 9:12	18.86	–	0.65	–
0: 5:12.7	16:16:49	21.09	–	0.59	–
0: 5:12.8	16: 9: 7	18.19	–	0.39	–
0: 5:13.1	16:11: 9	20.98	–	0.48	–
0: 5:13.3	16:15:48	22.23	–	0.66	–
0: 5:13.7	16:14:29	20.30	–	0.64	–
0: 5:13.7	16:15:14	22.53	–	1.09	–
0: 5:14.0	16: 9: 1	22.11	–	0.19	–
0: 5:14.1	16:12: 3	23.73	–	2.19	–
0: 5:14.1	16:13: 8	22.16	–	1.28	–
0: 5:14.3	16:17: 5	20.64	–	0.45	–
0: 5:14.4	16: 9:41	21.61	–	0.55	–
0: 5:14.5	16:14:45	21.87	–	0.67	–
0: 5:14.6	16:12:54	20.48	–	0.65	–
0: 5:14.6	16:13: 3	19.54	–	0.69	–
0: 5:14.8	16:17:38	20.82	–	0.56	–
0: 5:14.9	16:13: 0	19.63	–	0.62	–
0: 5:15.1	16:16:24	20.41	–	0.54	–
0: 5:15.3	16:10:30	22.88	–	1.28	–
0: 5:15.4	16:14: 0	23.25	–	2.20	–
0: 5:15.4	16:14:14	22.72	–	0.64	–
0: 5:15.5	16:14:41	22.87	–	0.97	–
0: 5:15.6	16: 8: 1	21.42	–	0.23	–
0: 5:15.6	16:13:44	19.91	–	0.62	–
0: 5:15.9	16:16:17	18.43	–	0.60	–
0: 5:16.1	16:13: 9	23.16	–	1.29	–
0: 5:16.2	16:11:23	19.60	–	0.47	–
0: 5:16.2	16:15:51	21.90	–	0.42	–
0: 5:16.5	16: 9: 7	23.14	–	-0.46	–
0: 5:16.5	16:12:27	25.72	–	2.99	–
0: 5:16.6	16:15: 4	21.64	–	0.70	–
0: 5:16.7	16: 9:17	21.17	–	0.45	–
0: 5:16.7	16:10:33	22.05	–	0.28	–
0: 5:16.8	16:17:18	20.70	–	0.36	–
0: 5:16.9	16:15:35	22.28	–	0.42	–
0: 5:17.1	16:10:16	21.81	–	0.51	–
0: 5:17.1	16:14:27	24.23	–	1.46	–
0: 5:17.2	16:10:31	21.15	–	0.47	–
0: 5:17.4	16: 8:50	22.66	–	-0.22	–
0: 5:17.4	16:11:11	22.04	–	0.36	–
0: 5:17.4	16:13:42	21.82	–	1.55	–
0: 5:17.5	16:12: 6	22.51	–	0.83	–
0: 5:17.7	16:14:35	18.17	–	0.71	–
0: 5:17.8	16:13:46	20.94	–	0.73	–
0: 5:17.8	16:14:45	18.47	–	0.67	–
0: 5:17.8	16:15:26	21.53	–	1.02	–
0: 5:18.1	16: 8:20	21.09	–	0.50	–
0: 5:18.1	16:10:42	19.95	–	0.39	–
0: 5:18.2	16:13: 2	21.68	–	0.79	–
0: 5:18.2	16:15: 2	22.45	–	0.54	–
0: 5:18.3	16:13:30	20.31	–	0.70	–
0: 5:18.3	16:16:30	19.79	–	0.57	–
0: 5:18.4	16:10: 7	20.69	–	0.51	–
0: 5:18.4	16:12:56	23.71	–	1.49	–
0: 5:18.5	16:11:25	21.74	–	0.62	–
0: 5:18.5	16:12:20	24.16	–	1.91	–
0: 5:18.5	16:12:43	24.50	–	2.23	–
0: 5:18.8	16:16:20	21.25	–	0.80	–
0: 5:18.9	16: 9: 5	19.12	–	0.56	–
0: 5:19.0	16:13:54	23.57	–	1.65	–
0: 5:19.2	16:10:29	18.97	–	0.25	–
0: 5:19.6	16:12: 2	22.80	–	0.79	–
0: 5:20.0	16: 9:56	20.23	–	0.77	–
0: 5:20.1	16:17:43	20.59	–	0.35	–
0: 5:20.2	16: 8:25	17.80	–	0.61	–

MS0002					contd.
RA(2000)	Dec(2000)	V	B-V	V-R	R-I
0: 5:20.5	16: 9: 1	18.13	–	0.64	–
0: 5:20.5	16:11:22	21.50	–	0.40	–
0: 5:20.5	16:14:30	23.54	–	1.03	–
0: 5:20.8	16: 9:15	22.07	–	0.55	–
0: 5:20.8	16: 9:33	21.43	–	0.39	–
0: 5:20.8	16:17:14	19.05	–	0.46	–
0: 5:20.9	16: 9: 1	20.21	–	0.91	–
0: 5:20.9	16:12:29	21.68	–	1.55	–
0: 5:21.0	16:12: 7	19.58	–	0.64	–
0: 5:21.1	16:14:37	23.25	–	1.14	–
0: 5:21.2	16:10:20	18.91	–	0.63	–
0: 5:21.2	16:15:38	20.51	–	0.59	–
0: 5:21.4	16:11: 6	18.65	–	0.54	–
0: 5:21.7	16: 9: 2	18.95	–	0.60	–
0: 5:21.9	16:13:18	20.85	–	0.62	–
0: 5:22.0	16:13:10	18.35	–	0.69	–
0: 5:22.1	16:14:11	20.89	–	0.47	–
0: 5:22.3	16:10:45	18.33	–	0.42	–
0: 5:22.7	16:17: 9	18.89	–	0.51	–
0: 5:22.8	16:12:59	18.80	–	0.69	–
0: 5:22.8	16:16:55	20.99	–	0.73	–
0: 5:23.0	16:11:56	22.64	–	0.59	–
0: 5:23.1	16:10:10	20.58	–	0.55	–
0: 5:23.1	16:10:25	19.72	–	0.74	–
0: 5:23.1	16:17: 6	19.83	–	0.66	–
0: 5:23.2	16:11:42	19.10	–	0.47	–
0: 5:23.4	16:12:49	20.51	–	0.70	–
0: 5:23.4	16:16:31	20.81	–	0.52	–
0: 5:23.4	16:16:35	21.05	–	0.65	–
0: 5:23.8	16:11:47	19.41	–	0.66	–
0: 5:23.9	16:15:13	20.15	–	0.35	–
0: 5:24.0	16:10:44	20.16	–	0.53	–
0: 5:24.0	16:13: 9	16.53	–	0.69	–
0: 5:24.0	16:13:18	18.99	–	0.74	–
0: 5:24.1	16:11:10	19.55	–	0.58	–
0: 5:24.1	16:12:11	22.38	–	0.21	–
0: 5:24.1	16:15:19	21.27	–	0.63	–
0: 5:24.2	16:11:19	20.54	–	0.67	–
0: 5:24.5	16:14:16	20.55	–	0.62	–
0: 5:25.0	16: 8:13	19.29	–	1.12	–
0: 5:25.0	16: 9: 2	24.25	–	-0.26	–
0: 5:25.0	16:13:28	20.40	–	0.64	–
0: 5:25.0	16:14:40	21.70	–	0.24	–
0: 5:25.4	16:13:46	20.33	–	1.03	–
0: 5:25.5	16:11:11	22.40	–	1.11	–
0: 5:25.5	16:15:13	21.50	–	0.58	–
0: 5:25.6	16: 9:51	23.06	–	-1.24	–
0: 5:25.6	16:13:29	21.50	–	0.67	–
0: 5:25.6	16:14:27	20.59	–	0.98	–
0: 5:25.7	16: 9:24	20.58	–	0.72	–
0: 5:25.8	16:12:35	22.83	–	0.61	–
0: 5:25.9	16:12: 0	21.82	–	0.89	–
0: 5:25.9	16:13:40	21.40	–	0.86	–
0: 5:25.9	16:17:33	20.70	–	0.42	–
0: 5:26.1	16:13:19	21.44	–	0.84	–
0: 5:26.1	16:13:30	21.42	–	0.76	–
0: 5:26.2	16: 9:32	23.09	–	1.11	–
0: 5:26.2	16:10: 3	18.39	–	0.60	–
0: 5:26.2	16:15:39	21.38	–	0.72	–
0: 5:26.2	16:16:53	20.18	–	0.45	–
0: 5:26.6	16:17:15	21.14	–	0.28	–
0: 5:26.7	16: 9:21	22.57	–	0.58	–
0: 5:26.7	16:12:32	21.61	–	0.84	–
0: 5:26.9	16:11:53	19.43	–	0.67	–
0: 5:26.9	16:15:12	21.77	–	0.25	–
0: 5:27.0	16:11:31	25.54	–	1.98	–

MS0002					contd.
RA(2000)	Dec(2000)	V	B-V	V-R	R-I
0: 5:27.0	16:13:17	20.16	–	0.64	–
0: 5:27.3	16:10:22	22.64	–	0.41	–
0: 5:27.4	16: 9:35	22.86	–	0.48	–
0: 5:27.4	16:16:57	21.39	–	0.55	–
0: 5:27.6	16:12:58	20.27	–	0.60	–
0: 5:27.6	16:14:54	19.12	–	0.68	–
0: 5:27.7	16: 8: 5	17.97	–	0.60	–
0: 5:27.7	16:11:27	21.40	–	0.99	–
0: 5:27.9	16: 8:16	19.50	–	0.46	–
0: 5:27.9	16:12:32	24.14	–	1.62	–
0: 5:27.9	16:12:48	22.48	–	0.80	–
0: 5:28.0	16:16:19	21.14	–	0.22	–
0: 5:28.4	16:14: 2	18.20	–	0.70	–
0: 5:28.5	16:10:46	20.04	–	0.29	–
0: 5:28.8	16: 9:11	20.92	–	0.28	–
0: 5:28.8	16:10:31	19.41	–	0.44	–
0: 5:28.8	16:11:51	21.18	–	0.71	–
0: 5:28.8	16:12:55	23.05	–	1.12	–
0: 5:28.9	16:13:30	20.52	–	0.72	–
0: 5:28.9	16:14: 8	21.34	–	0.67	–
0: 5:28.9	16:14:34	21.44	–	0.60	–
0: 5:29.0	16:14:46	22.27	–	0.49	–
0: 5:29.0	16:16:22	21.46	–	0.41	–
0: 5:29.1	16:15: 5	22.16	–	0.19	–
0: 5:29.3	16:12:23	18.87	–	0.65	–
0: 5:29.4	16:13:58	21.17	–	1.30	–
0: 5:29.4	16:17:40	20.68	–	0.76	–
0: 5:29.5	16: 8:27	21.60	–	0.19	–
0: 5:29.7	16:14:16	21.98	–	0.56	–
0: 5:29.8	16:13:47	22.21	–	0.49	–
0: 5:29.9	16:13:57	19.43	–	0.65	–
0: 5:30.0	16: 8:43	21.93	–	-0.14	–
0: 5:30.0	16:12:19	21.81	–	0.73	–
0: 5:30.1	16:13: 7	17.83	–	0.66	–
0: 5:30.1	16:16:37	18.26	–	0.61	–
0: 5:30.2	16:11:48	20.52	–	0.82	–
0: 5:30.4	16:14:40	20.73	–	0.21	–
0: 5:30.6	16:12: 4	21.85	–	0.68	–
0: 5:30.7	16:17:15	21.03	–	0.35	–
0: 5:30.8	16:13:10	20.27	–	0.72	–
0: 5:30.8	16:17:17	21.00	–	0.36	–
0: 5:31.0	16:12: 7	21.57	–	0.40	–
0: 5:31.1	16:11:49	18.53	–	0.73	–
0: 5:31.2	16:16:18	20.65	–	0.81	–
0: 5:31.4	16:12:22	22.00	–	1.15	–
0: 5:31.5	16: 8:52	22.20	–	-0.53	–
0: 5:31.5	16:16:27	21.40	–	0.11	–
0: 5:31.5	16:16:46	21.43	–	0.42	–
0: 5:31.7	16:12:47	24.78	–	2.96	–
0: 5:31.7	16:13:51	20.04	–	0.68	–
0: 5:31.7	16:14: 3	21.88	–	0.78	–
0: 5:31.7	16:17:27	18.73	–	1.18	–
0: 5:31.8	16:14:59	18.80	–	0.52	–
0: 5:32.0	16: 8:57	21.00	–	0.13	–
0: 5:32.0	16: 9:45	21.10	–	0.54	–
0: 5:32.0	16:10:10	21.61	–	0.15	–
0: 5:32.1	16: 9:26	23.46	–	0.79	–
0: 5:32.2	16:13: 8	22.24	–	0.87	–
0: 5:32.3	16:14: 4	20.43	–	0.75	–
0: 5:32.3	16:14:31	20.67	–	0.68	–
0: 5:32.3	16:14:54	20.17	–	0.90	–
0: 5:32.3	16:16:55	20.98	–	0.25	–
0: 5:32.4	16:10:53	19.90	–	0.60	–
0: 5:32.5	16: 9:19	21.01	–	0.89	–
0: 5:32.7	16: 8: 8	21.82	–	0.07	–
0: 5:32.7	16:10:26	20.21	–	0.56	–

MS0002					contd.
RA(2000)	Dec(2000)	V	B-V	V-R	R-I
0: 5:32.8	16: 8:49	21.35	–	0.40	–
0: 5:33.0	16:12: 0	20.52	–	0.51	–
0: 5:33.1	16:14:21	20.69	–	0.67	–
0: 5:33.1	16:16: 8	21.45	–	0.24	–
0: 5:33.2	16: 9:53	22.96	–	-0.26	–
0: 5:33.3	16: 8:46	22.79	–	0.61	–
0: 5:33.5	16:12:41	20.23	–	0.76	–
0: 5:33.5	16:16:53	21.22	–	0.29	–
0: 5:33.5	16:17: 5	21.40	–	0.57	–
0: 5:33.7	16:14:26	19.53	–	0.78	–
0: 5:33.8	16:11: 9	20.01	–	1.22	–
0: 5:33.8	16:12:37	22.80	–	0.98	–
0: 5:33.9	16:12: 8	21.81	–	0.37	–
0: 5:34.0	16:15: 6	18.76	–	0.65	–
0: 5:34.0	16:16:56	20.61	–	0.37	–
0: 5:34.2	16: 9:24	23.06	–	0.73	–
0: 5:34.3	16:11:49	23.00	–	0.05	–
0: 5:34.3	16:12:22	19.62	–	0.55	–
0: 5:34.3	16:14:18	21.51	–	0.74	–
0: 5:34.4	16:14: 3	18.77	–	0.64	–
0: 5:34.5	16:13:41	22.09	–	0.49	–
0: 5:34.6	16: 8:45	22.63	–	-0.10	–
0: 5:34.8	16:10:54	20.49	–	0.88	–
0: 5:34.8	16:14: 1	20.87	–	0.66	–
0: 5:35.1	16: 8:54	21.31	–	0.28	–
0: 5:35.3	16:17:48	18.73	–	0.77	–
0: 5:35.4	16:14:38	19.92	–	0.59	–
0: 5:36.1	16:16:14	19.95	–	0.44	–
0: 5:36.1	16:16:42	19.91	–	0.53	–
0: 5:36.3	16: 8:24	20.82	–	0.17	–
0: 5:36.5	16:15:41	21.02	–	0.16	–
0: 5:36.7	16:12:35	19.44	–	0.61	–
0: 5:36.9	16:11:17	19.57	–	1.13	–
0: 5:37.2	16:13:47	18.26	–	0.63	–
0: 5:37.3	16:14: 5	21.67	–	0.38	–
0: 5:37.3	16:15:32	21.35	–	0.68	–
0: 5:37.6	16: 9:21	19.47	–	0.29	–
0: 5:37.8	16: 8:59	20.62	–	0.42	–
0: 5:37.8	16:11:36	22.26	–	0.60	–
0: 5:37.8	16:13:38	17.81	–	0.64	–
0: 5:37.8	16:14:40	21.29	–	0.48	–
0: 5:38.0	16:16:42	18.75	–	0.54	–
0: 5:38.1	16:12:30	19.85	–	0.33	–
0: 5:38.1	16:13:28	19.95	–	0.51	–
0: 5:38.1	16:14:50	22.40	–	0.16	–
0: 5:38.1	16:15: 3	22.27	–	1.06	–
0: 5:38.4	16:10:45	18.04	–	0.62	–
0: 5:38.5	16:12:47	22.21	–	0.20	–
0: 5:38.6	16:10:23	20.67	–	0.53	–
0: 5:38.6	16:15:12	19.55	–	0.55	–
0: 5:38.7	16: 9:14	22.61	–	-0.23	–
0: 5:38.7	16:11:50	22.25	–	1.15	–
0: 5:38.8	16:11:59	20.87	–	0.50	–
0: 5:39.0	16:15: 6	21.77	–	0.74	–
0: 5:39.3	16:10:25	22.91	–	-1.93	–
0: 5:39.3	16:15:59	21.00	–	0.42	–
0: 5:39.7	16:14:52	20.94	–	0.71	–
0: 5:39.7	16:17:19	20.91	–	0.41	–
0: 5:39.8	16:17:46	21.28	–	0.35	–
0: 5:39.9	16:16:42	19.74	–	0.50	–
0: 5:40.1	16: 8:57	21.78	–	-1.47	–
0: 5:40.1	16:15:48	20.34	–	0.43	–
0: 5:40.5	16:15: 8	21.19	–	0.27	–
0: 5:40.6	16:14:45	21.24	–	0.11	–
0: 5:40.7	16: 9:39	20.83	–	0.38	–
0: 5:40.8	16:12:19	18.55	–	0.59	–

MS0002					contd.
RA(2000)	Dec(2000)	V	B-V	V-R	R-I
0: 5:41.0	16:15:19	21.26	–	0.23	–
0: 5:41.2	16: 9:51	20.22	–	0.95	–
0: 5:41.4	16:11:11	22.25	–	-0.08	–
0: 5:41.4	16:14:41	21.96	–	0.51	–
0: 5:41.7	16:11:35	20.20	–	0.95	–
0: 5:41.7	16:15:26	19.80	–	0.51	–
0: 5:41.8	16: 9:47	20.56	–	0.55	–
0: 5:43.0	16:17:33	20.06	–	0.43	–
0: 5:43.1	16:15: 2	21.79	–	-0.13	–
0: 5:43.1	16:17:39	18.67	–	0.65	–
0: 5:43.3	16:12:19	21.93	–	0.56	–
0: 5:43.3	16:16:17	17.14	–	0.60	–
0: 5:43.4	16: 9:54	22.01	–	-0.75	–
0: 5:43.5	16:10: 3	20.20	–	0.81	–
0: 5:43.5	16:11: 7	21.46	–	0.66	–
0: 5:43.6	16:12:46	19.85	–	0.31	–
0: 5:43.7	16:11:37	21.23	–	0.46	–
0: 5:43.8	16:10:28	21.58	–	0.76	–
0: 5:44.0	16:12:17	19.74	–	0.56	–
0: 5:44.0	16:15:43	20.51	–	0.40	–
0: 5:44.1	16:13:43	21.74	–	0.10	–
0: 5:44.3	16:16:46	21.19	–	0.02	–
0: 5:44.7	16: 8:39	21.37	–	-0.27	–
0: 5:44.7	16:17:45	20.38	–	0.09	–
0: 5:44.8	16: 9:17	22.09	–	0.40	–
0: 5:45.0	16:13:37	20.57	–	0.52	–
0: 5:45.1	16: 8:53	18.33	–	0.32	–
0: 5:45.1	16:14:37	19.50	–	1.06	–
0: 5:45.3	16:12: 5	18.98	–	1.29	–
0: 5:45.4	16: 9:51	20.02	–	0.41	–
0: 5:45.7	16: 8:34	20.98	–	-0.27	–

Table 8. Catalog of galaxies in the field of MS 0301+1516.

RA(2000)	Dec(2000)	V	B-V	V-R	R-I
3: 4:10.9	15:22:59	19.46	–	0.55	–
3: 4:11.7	15:28:10	18.49	0.31	0.64	0.63
3: 4:12.4	15:25:42	17.40	0.69	0.61	1.00
3: 4:12.6	15:25:35	19.46	-0.15	1.01	1.23
3: 4:12.6	15:31: 9	19.26	0.38	0.82	0.53
3: 4:13.6	15:25:15	18.38	0.77	0.81	1.22
3: 4:13.7	15:23:54	17.83	0.82	0.45	1.54
3: 4:13.9	15:31: 9	18.77	0.49	0.67	0.77
3: 4:14.3	15:29:21	19.66	0.21	0.80	0.04
3: 4:14.3	15:30: 9	18.82	0.26	0.68	0.84
3: 4:14.5	15:24:57	18.40	0.83	0.78	1.15
3: 4:15.1	15:28:50	17.18	0.86	0.48	0.76
3: 4:15.4	15:26:31	18.54	0.15	0.53	0.58
3: 4:15.4	15:27:54	17.19	0.85	0.46	0.84
3: 4:15.5	15:31:28	21.82	–	1.43	0.45
3: 4:15.6	15:23:30	18.10	0.76	0.19	1.63
3: 4:16.0	15:29:42	16.74	0.92	0.49	0.84
3: 4:16.4	15:26: 5	20.42	-0.73	1.31	0.52
3: 4:16.6	15:26:54	18.63	0.12	0.21	1.17
3: 4:16.6	15:27: 5	17.96	0.04	0.04	1.13
3: 4:16.9	15:25:53	19.77	-0.27	0.72	0.08
3: 4:16.9	15:29:39	20.54	-0.27	0.79	-0.29
3: 4:17.2	15:28:50	20.15	0.10	0.97	1.01
3: 4:17.3	15:29:51	21.14	-0.06	1.02	-0.68
3: 4:17.4	15:23: 7	19.15	–	-0.04	–
3: 4:17.6	15:26:12	19.59	-0.02	0.49	0.47
3: 4:17.7	15:27:41	17.97	0.16	0.03	1.27
3: 4:17.9	15:26:31	18.57	0.43	0.47	0.77
3: 4:18.0	15:29:36	21.89	-0.84	1.44	1.27
3: 4:18.3	15:29:43	19.11	0.56	0.46	0.72
3: 4:18.4	15:25:30	20.47	-0.81	1.07	-0.15
3: 4:18.4	15:26:11	19.32	0.37	0.60	0.45
3: 4:18.7	15:28:27	20.25	-0.03	0.64	0.65
3: 4:18.9	15:30:47	17.99	0.12	0.15	0.81
3: 4:19.1	15:26:48	18.66	0.41	0.34	0.83
3: 4:19.1	15:30:28	20.22	–	1.04	1.69
3: 4:19.2	15:28:58	21.06	-0.44	0.44	0.38
3: 4:19.3	15:22:53	17.81	–	-0.27	–
3: 4:19.3	15:24:31	18.56	0.27	0.47	0.89
3: 4:19.3	15:27:30	18.03	0.51	-0.13	1.23
3: 4:19.5	15:28:37	21.23	-0.15	0.87	0.83
3: 4:19.8	15:26:31	19.65	0.08	0.43	0.33
3: 4:19.8	15:29: 7	18.84	0.55	0.39	0.67
3: 4:19.9	15:26:41	19.17	0.44	0.49	0.78
3: 4:20.3	15:31:45	20.20	–	0.67	1.72
3: 4:20.4	15:26:48	19.74	-0.03	0.60	0.79
3: 4:20.4	15:31: 8	19.24	0.89	0.62	1.22
3: 4:20.5	15:28:41	21.24	-0.84	0.49	-0.46
3: 4:20.9	15:27:56	20.25	0.50	0.50	0.80
3: 4:21.0	15:28:18	19.97	0.55	0.39	0.76
3: 4:21.2	15:26:41	20.38	-0.05	0.61	0.05
3: 4:21.2	15:28:52	20.40	0.50	0.09	1.00
3: 4:21.3	15:29:49	20.85	0.29	0.29	-0.88
3: 4:21.6	15:28:54	20.91	-0.36	0.32	-0.44
3: 4:21.8	15:27:30	17.43	0.62	0.39	0.82
3: 4:21.9	15:22:52	18.86	–	-0.41	–
3: 4:22.2	15:25:51	16.45	1.01	0.52	0.78
3: 4:22.5	15:25:35	18.70	0.47	0.39	0.47
3: 4:22.7	15:27: 4	20.45	-0.15	0.33	-0.25
3: 4:22.8	15:25:47	16.93	1.06	0.47	0.79
3: 4:22.9	15:22:27	19.27	–	-0.21	–
3: 4:23.4	15:24:16	20.25	-0.55	0.89	0.51
3: 4:23.6	15:25:34	21.01	-0.53	0.93	-1.70
3: 4:23.6	15:30:19	18.09	0.83	0.38	0.86
3: 4:23.7	15:29:25	20.19	0.39	-0.11	2.02
3: 4:23.8	15:24:57	20.94	-0.47	1.37	0.20

MS0301					contd.
RA(2000)	Dec(2000)	V	B-V	V-R	R-I
3: 4:24.0	15:30: 1	20.05	0.38	0.22	0.16
3: 4:24.2	15:24:50	21.14	-0.47	1.56	0.21
3: 4:24.3	15:26:50	20.30	0.05	0.28	0.16
3: 4:24.3	15:27:59	19.38	0.48	0.11	0.62
3: 4:24.3	15:28: 5	18.27	0.82	0.37	0.78
3: 4:24.5	15:26:52	19.87	0.09	0.26	0.17
3: 4:25.6	15:27:59	20.24	0.29	-0.04	1.24
3: 4:25.6	15:28:40	21.08	0.10	0.88	-0.17
3: 4:25.7	15:27:35	20.68	-0.01	0.56	-0.01
3: 4:26.0	15:24:33	19.09	0.41	0.37	-0.08
3: 4:26.1	15:26: 9	17.20	0.84	0.41	0.75
3: 4:26.1	15:26:45	17.39	0.90	0.46	0.84
3: 4:26.1	15:28: 3	18.44	1.36	0.50	0.96
3: 4:26.6	15:27:57	20.20	0.37	0.53	0.29
3: 4:26.8	15:27:11	19.37	0.63	0.19	0.60
3: 4:27.2	15:28:49	17.41	0.94	0.40	0.86
3: 4:27.4	15:27:29	19.18	0.77	0.37	0.95
3: 4:27.4	15:29: 3	19.10	0.73	0.28	1.00
3: 4:27.7	15:27:33	20.57	0.31	0.50	1.42
3: 4:27.8	15:23:27	19.92	0.54	1.07	1.13
3: 4:28.1	15:30:22	20.02	0.41	0.20	0.19
3: 4:28.4	15:28:14	16.19	0.98	0.45	0.87
3: 4:28.4	15:31:50	19.71	–	0.07	–
3: 4:28.6	15:29:21	20.65	0.13	0.63	0.07
3: 4:28.8	15:28:37	18.59	0.46	0.84	0.05
3: 4:28.9	15:28:17	18.88	1.29	0.43	1.15
3: 4:29.0	15:27:46	19.69	0.72	0.30	1.06
3: 4:29.0	15:28: 5	19.93	0.51	0.12	1.53
3: 4:29.0	15:28:11	18.95	1.32	0.32	0.98
3: 4:29.4	15:28:24	18.06	1.52	0.49	0.95
3: 4:29.4	15:30: 6	20.09	0.45	0.28	0.34
3: 4:29.5	15:22:49	19.01	1.47	0.52	0.70
3: 4:29.6	15:28: 9	18.38	0.90	0.40	0.86
3: 4:29.6	15:29:34	20.17	0.74	0.44	0.22
3: 4:29.7	15:30:21	18.82	1.64	0.42	1.02
3: 4:30.1	15:27:34	15.76	1.01	0.46	0.88
3: 4:30.1	15:30:55	19.66	0.99	-0.11	1.41
3: 4:30.3	15:28:44	18.62	0.99	0.28	0.92
3: 4:30.4	15:25: 2	21.20	-0.32	0.92	-0.14
3: 4:30.6	15:29:17	18.70	1.18	0.32	0.95
3: 4:30.7	15:29:31	20.83	0.34	0.52	-0.01
3: 4:30.8	15:25:53	20.43	0.62	0.41	-0.60
3: 4:31.0	15:23:31	21.20	-0.15	1.29	-0.19
3: 4:31.1	15:30:58	20.62	0.49	0.53	0.63
3: 4:31.3	15:27:44	19.17	0.96	0.22	0.97
3: 4:31.3	15:30:20	17.27	0.63	0.39	0.81
3: 4:31.6	15:31:14	20.76	-0.75	1.19	0.48
3: 4:32.0	15:29:12	18.61	1.02	0.31	0.85
3: 4:32.1	15:25:45	18.96	0.94	0.37	0.57
3: 4:32.2	15:28:23	20.91	0.31	0.57	0.15
3: 4:32.3	15:29:47	18.66	1.28	0.41	0.95
3: 4:32.3	15:31:20	17.97	0.71	0.26	0.83
3: 4:32.8	15:29: 5	21.44	-0.14	1.15	0.01
3: 4:33.7	15:26:41	18.60	1.42	0.47	0.98
3: 4:33.8	15:28:42	19.85	1.27	0.35	0.38
3: 4:33.9	15:32:26	19.42	–	-0.06	–
3: 4:34.1	15:26:43	18.43	1.34	0.39	0.90
3: 4:34.4	15:23:57	21.08	1.04	1.24	0.08
3: 4:34.8	15:27:53	19.95	0.69	-0.43	1.13
3: 4:34.9	15:29:59	20.94	0.00	0.30	0.18
3: 4:35.1	15:29:17	16.99	0.97	0.41	0.78
3: 4:35.4	15:25: 8	20.86	0.35	0.97	0.29
3: 4:35.6	15:25:15	18.68	1.98	0.53	0.65
3: 4:35.7	15:24:50	20.25	1.44	0.63	0.39
3: 4:36.1	15:32:18	18.38	–	0.17	0.88
3: 4:36.7	15:29:53	21.31	0.87	0.85	0.16

MS0301					contd.
RA(2000)	Dec(2000)	V	B-V	V-R	R-I
3: 4:36.9	15:23:31	20.53	0.87	0.62	-0.85
3: 4:36.9	15:31:54	20.19	–	0.35	–
3: 4:37.3	15:24:14	20.97	0.78	0.55	0.89
3: 4:37.4	15:30:36	21.04	1.26	1.19	0.91
3: 4:37.5	15:25:50	20.86	0.81	0.75	0.61
3: 4:37.6	15:27:40	20.34	-0.12	0.30	0.31
3: 4:37.7	15:25:14	19.43	1.04	0.19	0.43
3: 4:37.8	15:31:14	20.44	1.16	0.49	1.49
3: 4:38.0	15:31:37	21.29	0.80	0.86	0.88
3: 4:38.1	15:27:16	20.35	1.60	0.66	1.37
3: 4:38.1	15:29:21	20.93	0.45	0.40	0.21
3: 4:38.9	15:29:26	20.86	1.34	1.14	0.80
3: 4:39.0	15:30:46	21.94	0.08	1.83	0.77
3: 4:39.3	15:22:51	20.63	1.47	0.63	-0.08
3: 4:39.6	15:28:24	19.64	0.87	-0.51	0.74
3: 4:39.9	15:31: 6	20.37	0.80	0.51	0.28
3: 4:40.0	15:26:16	21.13	-0.31	0.51	0.01
3: 4:40.1	15:26:52	20.22	0.54	0.32	0.62
3: 4:40.1	15:29:30	20.83	1.27	1.09	0.83
3: 4:40.4	15:30:42	20.98	0.87	1.02	0.78
3: 4:40.9	15:30:19	21.43	-0.38	0.90	-0.57
3: 4:41.0	15:27:49	20.28	1.13	0.57	0.77
3: 4:41.3	15:22:48	19.15	0.57	0.29	0.71
3: 4:41.4	15:31:44	20.22	0.07	0.04	-0.45
3: 4:42.3	15:26:34	20.16	0.83	0.47	0.72
3: 4:42.7	15:29:13	21.25	1.16	1.04	0.67
3: 4:43.0	15:27:46	20.29	1.54	0.98	0.95
3: 4:43.1	15:30:58	19.56	0.43	0.43	0.26
3: 4:43.3	15:29: 5	18.78	0.72	-0.21	-0.03
3: 4:43.4	15:29:10	20.25	0.64	0.33	0.39
3: 4:44.0	15:31:59	19.49	0.65	0.16	0.15
3: 4:44.1	15:31:49	20.31	1.48	0.85	0.73
3: 4:44.2	15:29: 9	20.40	1.26	0.90	0.80
3: 4:44.6	15:22:58	19.59	1.05	0.10	0.09
3: 4:44.9	15:29:12	20.06	0.62	0.29	0.43
3: 4:45.3	15:28:47	19.34	0.83	0.38	0.65
3: 4:45.3	15:32:22	20.58	0.72	0.27	-0.51
3: 4:45.7	15:22:32	20.17	3.02	0.04	-0.19
3: 4:45.8	15:28:26	20.57	1.58	1.03	0.93
3: 4:46.0	15:28:13	20.69	1.00	1.09	0.78
3: 4:46.4	15:28:36	18.79	0.51	-0.75	0.65
3: 4:46.5	15:29:16	20.55	1.17	0.91	0.66
3: 4:46.7	15:28:22	20.44	0.33	0.27	0.48
3: 4:46.8	15:28:31	20.59	0.64	0.76	0.80
3: 4:47.2	15:28:58	21.24	–	1.01	0.77
3: 4:47.4	15:25:13	19.13	0.70	0.16	1.15
3: 4:47.4	15:29: 3	21.02	2.23	0.85	0.52
3: 4:47.6	15:22:58	18.99	0.71	0.10	0.59
3: 4:47.6	15:28:47	20.10	1.08	0.65	0.79
3: 4:47.9	15:26:15	22.45	0.72	1.38	0.18
3: 4:48.2	15:28:24	20.74	2.54	0.96	0.89
3: 4:48.3	15:23:27	20.18	0.55	-0.10	0.57
3: 4:48.5	15:31:34	20.34	0.86	0.50	0.32
3: 4:48.6	15:30:46	18.99	1.25	0.39	0.52
3: 4:49.1	15:28: 6	21.59	0.32	0.98	0.33
3: 4:49.5	15:29:35	20.11	1.00	0.28	0.38
3: 4:49.7	15:28:14	18.91	0.62	0.17	0.54
3: 4:49.8	15:27:57	20.60	0.96	0.48	0.38
3: 4:49.8	15:31:26	19.03	0.55	0.12	0.22
3: 4:50.0	15:31:56	19.90	0.54	0.23	-1.48
3: 4:50.1	15:29:23	18.88	1.51	-0.57	0.70
3: 4:50.1	15:29:28	19.78	0.71	0.22	0.27
3: 4:50.1	15:31:10	20.39	1.50	0.70	0.45
3: 4:50.4	15:26:18	20.46	0.80	0.60	0.42
3: 4:50.8	15:26:14	17.94	1.66	0.26	0.02
3: 4:50.8	15:27:48	20.52	1.29	0.46	0.50

MS0301					contd.
RA(2000)	Dec(2000)	V	B-V	V-R	R-I
3: 4:51.0	15:27:13	21.33	–	1.06	0.24
3: 4:51.1	15:31:21	17.54	1.52	0.22	0.52
3: 4:51.7	15:29:24	22.13	0.98	0.09	-1.27
3: 4:51.9	15:29: 0	20.88	0.65	0.18	-0.68
3: 4:51.9	15:31: 7	19.79	1.28	0.60	0.66
3: 4:52.1	15:27:14	20.38	0.40	0.96	0.71
3: 4:52.1	15:28:27	19.99	0.65	0.11	0.19
3: 4:52.5	15:26:25	21.02	0.47	0.07	-0.24
3: 4:52.6	15:22:56	18.29	1.44	0.42	0.84
3: 4:52.6	15:24:52	17.94	0.79	0.26	0.68
3: 4:52.7	15:32:10	18.68	–	0.40	0.42
3: 4:52.9	15:29: 7	19.16	1.42	0.44	0.63
3: 4:52.9	15:30:39	21.09	2.46	0.06	–
3: 4:52.9	15:31: 3	20.78	1.76	0.09	-0.14
3: 4:53.0	15:30:46	20.38	1.47	0.27	0.19
3: 4:53.8	15:31:21	19.71	–	-0.06	-0.09
3: 4:53.9	15:30:40	19.29	1.20	0.30	0.63
3: 4:54.6	15:31:51	18.09	–	0.37	0.09
3: 4:55.6	15:28: 1	18.94	1.68	0.51	0.70
3: 4:55.8	15:23:20	19.57	1.31	-0.27	0.20
3: 4:56.0	15:24:38	18.36	1.53	0.31	0.84
3: 4:56.3	15:22:32	18.75	0.92	-0.01	0.64
3: 4:56.3	15:22:57	16.96	1.00	0.35	0.86
3: 4:57.7	15:22:43	19.79	1.71	-0.04	1.03
3: 4:58.8	15:27:52	20.83	–	0.18	0.20
3: 4:59.0	15:27: 8	20.37	1.04	-0.14	-0.53

Table 9. Catalog of galaxies in the field of MS 0735+7421.

RA(2000)	Dec(2000)	V	B-V	V-R	R-I
7:40:39.1	74:16:19	20.84	1.47	0.64	0.81
7:40:44.7	74:14:36	20.57	0.37	0.02	0.08
7:40:45.6	74:16:31	21.61	1.10	0.70	1.41
7:40:48.0	74:13:31	22.05	1.72	0.70	2.23
7:40:49.0	74:10:24	20.65	1.43	1.00	0.82
7:40:50.8	74:12:38	21.22	1.80	1.19	1.24
7:40:51.6	74:11:38	22.28	0.92	1.05	0.93
7:40:51.7	74:15:34	21.94	1.49	1.51	1.21
7:40:52.4	74: 9:41	19.88	1.56	0.97	0.92
7:40:53.0	74:14: 7	21.30	1.43	1.54	1.20
7:40:53.3	74:17:42	19.66	1.68	0.93	3.14
7:40:53.8	74:12:52	22.94	–	2.06	1.58
7:40:53.8	74:17:11	21.51	1.21	1.10	-0.38
7:40:54.7	74:11:36	21.23	0.97	0.85	0.19
7:40:55.1	74:12:17	21.98	0.12	0.68	-2.78
7:40:56.4	74:14:46	22.19	2.94	1.14	0.58
7:40:56.4	74:15:24	21.39	0.75	1.18	0.58
7:40:57.3	74:15: 0	20.33	0.81	0.87	0.53
7:40:58.3	74: 9:29	21.41	0.93	1.65	0.44
7:40:59.6	74:17: 1	21.01	1.32	1.26	1.34
7:41: 1.0	74:11:41	21.08	2.23	0.88	1.07
7:41: 1.0	74:13: 8	22.09	0.38	1.46	0.73
7:41: 1.0	74:15:36	22.49	–	1.81	1.19
7:41: 1.5	74:12:30	19.24	0.96	0.81	0.57
7:41: 1.6	74:12:56	20.34	1.27	1.03	0.67
7:41: 1.7	74:16:40	20.50	1.57	0.96	0.84
7:41: 2.2	74:16: 8	20.76	4.01	1.23	0.97
7:41: 3.0	74:11:53	21.95	1.06	0.97	0.19
7:41: 5.4	74:17:10	22.35	0.75	1.42	1.19
7:41: 5.9	74:16:43	22.13	1.07	0.91	1.79
7:41: 6.3	74:14:58	19.89	1.65	0.95	0.71
7:41: 6.3	74:15: 4	20.31	2.29	0.78	0.73
7:41: 7.4	74:11:33	22.86	-0.78	1.59	0.25
7:41: 7.7	74:15: 2	20.93	1.72	1.03	0.55
7:41: 8.1	74:13: 4	20.39	1.26	1.07	0.75
7:41: 8.2	74:14:21	20.14	1.64	0.95	0.75
7:41: 9.2	74:12: 7	20.21	1.87	1.04	0.74
7:41:12.4	74:13:50	23.09	1.75	1.55	0.80
7:41:12.9	74:11:34	21.02	.23	0.88	0.62
7:41:13.0	74:17:52	21.85	0.43	0.94	-0.32
7:41:14.1	74:18:19	18.95	1.84	0.93	–
7:41:14.2	74:18:12	20.20	2.11	0.87	–
7:41:14.8	74:12: 7	22.22	0.72	1.05	0.65
7:41:15.2	74:14:26	21.48	1.50	1.52	1.34
7:41:15.7	74: 9:31	19.87	1.72	0.68	0.64
7:41:15.9	74:11:34	21.25	0.53	0.58	0.13
7:41:15.9	74:16:23	22.00	1.51	1.57	1.56
7:41:17.2	74:13:53	20.73	1.10	0.92	0.51
7:41:17.5	74:18:41	20.72	1.45	0.71	–
7:41:17.7	74:13:36	21.25	0.44	0.87	0.15
7:41:18.4	74:16:22	21.37	1.70	0.65	0.77
7:41:18.9	74:12:12	20.73	0.83	0.74	0.40
7:41:20.5	74:16:41	21.58	0.85	0.91	1.27
7:41:21.0	74:15:26	19.26	1.51	0.95	0.72
7:41:22.0	74:14:31	20.74	1.88	1.00	0.80
7:41:22.0	74:14:54	21.16	1.32	1.08	0.60
7:41:22.1	74:12:58	20.69	1.39	1.02	0.46
7:41:22.2	74: 9:45	20.39	2.00	1.69	1.78
7:41:25.0	74:12:53	19.89	1.47	0.95	0.74
7:41:25.8	74:18:10	21.15	1.35	1.11	–
7:41:25.9	74:17: 0	20.40	1.32	0.96	0.96
7:41:26.1	74:14:26	22.17	0.74	0.63	0.00
7:41:26.8	74:10: 0	22.62	1.04	1.87	0.73
7:41:27.2	74:10:33	20.86	1.04	0.78	0.41
7:41:28.6	74:17:25	21.73	0.60	1.35	0.98
7:41:30.4	74:16:43	19.62	1.78	0.94	0.85

MS0735					contd.
RA(2000)	Dec(2000)	V	B-V	V-R	R-I
7:41:31.1	74:17:57	19.75	1.44	0.91	2.43
7:41:31.3	74:18:30	19.47	1.69	0.79	–
7:41:31.5	74:12:55	19.72	1.66	0.96	0.74
7:41:32.4	74:10:45	21.68	1.44	1.26	1.24
7:41:33.7	74:15:18	21.05	1.89	1.18	0.56
7:41:34.7	74:11: 5	20.75	1.48	0.84	0.81
7:41:34.7	74:14:28	22.12	0.70	0.78	0.35
7:41:36.2	74:17:40	21.51	1.09	0.95	1.23
7:41:36.4	74:13:13	21.97	1.62	0.90	0.01
7:41:36.8	74:16: 9	21.05	1.46	0.96	0.97
7:41:36.9	74:16:40	21.25	1.92	0.97	1.22
7:41:37.1	74:16: 4	21.53	1.26	0.93	0.82
7:41:38.6	74:18:15	21.18	1.21	1.14	–
7:41:39.2	74:11:54	22.42	3.89	1.72	1.65
7:41:39.2	74:16:29	21.22	0.68	1.26	1.16
7:41:39.5	74:15:48	20.24	1.03	0.94	0.68
7:41:39.8	74:15:37	21.21	1.63	0.95	0.65
7:41:40.0	74:13:29	21.82	1.34	0.95	0.68
7:41:41.1	74:18:22	21.30	1.91	-0.80	–
7:41:42.0	74:10: 9	19.76	1.65	0.94	0.76
7:41:42.6	74:14:58	21.31	1.60	1.09	0.44
7:41:42.7	74:15:23	20.84	1.35	1.21	0.73
7:41:42.8	74:16:26	19.39	1.28	0.79	0.58
7:41:43.1	74:14:36	19.81	2.13	0.85	0.74
7:41:43.4	74:17:41	20.37	1.61	0.91	0.90
7:41:43.5	74:10:38	22.54	–	1.77	1.67
7:41:44.6	74:14:38	18.53	1.62	0.95	0.79
7:41:45.0	74:10:40	20.09	1.64	1.06	0.72
7:41:45.1	74:13:31	20.31	1.14	1.01	0.72
7:41:45.7	74:13:34	20.93	1.54	1.26	1.31
7:41:45.7	74:15:57	20.01	2.67	0.95	0.73
7:41:46.0	74:15: 4	21.15	1.02	1.15	0.45
7:41:46.1	74:14: 8	18.86	1.58	0.95	0.75
7:41:46.4	74:10:52	19.39	1.78	0.74	0.75
7:41:46.7	74:14:12	19.54	1.68	0.85	0.84
7:41:47.5	74:16:16	20.85	2.27	1.06	0.75
7:41:48.3	74:17:55	19.69	1.65	0.81	0.57
7:41:48.7	74:15:27	20.67	2.01	0.94	0.62
7:41:48.7	74:18: 3	21.08	1.34	0.97	2.44
7:41:48.9	74:13: 6	23.54	0.17	2.90	1.75
7:41:49.1	74:14:10	21.36	1.22	0.69	0.56
7:41:49.1	74:14:40	23.40	-0.52	2.36	0.93
7:41:49.2	74:18:43	20.86	1.96	0.88	–
7:41:49.6	74:12: 8	20.36	1.59	0.94	0.77
7:41:49.7	74:12:16	20.97	1.88	0.93	0.63
7:41:50.9	74:12:30	19.78	1.35	0.93	0.71
7:41:50.9	74:18:21	18.60	0.80	0.68	–
7:41:51.0	74:18:51	21.14	1.70	0.77	–
7:41:51.6	74:15:16	22.53	-0.56	1.22	0.68
7:41:52.2	74:10:53	20.71	2.94	0.60	0.47
7:41:52.4	74:12:13	19.53	1.91	0.91	0.75
7:41:53.2	74:12:12	19.86	2.24	0.83	0.79
7:41:53.3	74:17: 0	21.74	0.40	1.27	1.06
7:41:53.6	74:11: 0	20.73	2.60	0.75	0.57
7:41:53.7	74:18:14	22.58	0.91	1.56	–
7:41:53.9	74:15: 8	22.40	1.47	1.27	0.80
7:41:54.0	74:17:28	19.37	1.71	1.00	0.74
7:41:54.1	74:13:36	20.48	1.44	1.62	1.66
7:41:54.1	74:15:45	21.47	0.23	0.67	0.54
7:41:54.7	74: 9:32	21.11	0.50	0.77	0.80
7:41:54.7	74:14:16	19.49	1.36	0.93	0.74
7:41:55.0	74:11:54	21.10	1.24	0.47	0.91
7:41:55.3	74:18: 9	21.36	1.01	1.26	–
7:41:55.6	74:13:34	20.42	1.59	1.04	0.76
7:41:56.3	74:12: 8	20.44	3.15	1.00	0.84
7:41:56.4	74:13:41	20.62	2.65	0.89	0.75

MS0735					contd.
RA(2000)	Dec(2000)	V	B-V	V-R	R-I
7:41:56.5	74:11:53	19.90	1.59	0.93	0.77
7:41:57.3	74:13: 6	21.96	0.95	1.18	0.44
7:41:57.4	74:13:57	21.96	1.14	1.08	0.92
7:41:57.9	74:12:53	21.40	2.08	0.99	0.71
7:41:58.0	74:10:19	19.67	1.38	0.89	0.77
7:41:58.5	74: 9:33	20.04	1.83	0.90	0.64
7:41:58.7	74:16:45	19.74	2.10	0.91	0.73
7:41:58.9	74: 9:42	20.00	1.90	0.88	0.86
7:41:59.1	74:15:46	20.79	1.51	0.96	0.73
7:41:59.2	74:11:48	20.14	1.85	0.97	0.75
7:41:59.3	74:10:21	21.19	1.68	0.61	0.77
7:41:59.5	74: 9:51	19.38	1.75	0.90	0.74
7:41:59.6	74:12: 1	21.60	0.90	0.71	0.75
7:41:59.7	74:12:49	20.45	1.22	0.97	0.95
7:42: 2.6	74:11:30	22.58	0.66	1.27	1.31
7:42: 2.7	74:13:33	21.60	1.34	1.07	0.73
7:42: 3.3	74:15: 0	21.10	1.33	0.88	0.41
7:42: 3.8	74:17:22	20.65	1.32	0.91	0.34
7:42: 5.1	74:15:58	21.81	1.58	0.87	0.56
7:42: 5.8	74:13:12	20.85	1.11	0.99	0.66
7:42: 6.6	74:15:38	19.74	1.22	0.71	0.62
7:42: 6.8	74:17:18	21.51	1.85	1.39	0.78
7:42: 7.2	74:12:26	21.29	1.20	0.82	0.70
7:42: 8.5	74:10: 9	21.34	3.13	0.50	0.39
7:42: 8.8	74:10:48	21.42	1.38	0.67	0.71
7:42:10.4	74: 9:45	21.24	1.76	1.08	0.43
7:42:11.7	74:11:32	20.24	1.40	0.87	0.71
7:42:12.6	74:12:33	21.31	1.87	0.96	1.04
7:42:12.7	74:15:18	19.33	1.83	0.91	0.79
7:42:15.3	74:18:40	19.88	1.65	1.11	–
7:42:16.1	74: 9:43	19.76	2.46	1.03	0.77
7:42:17.0	74: 9:34	21.48	2.03	1.49	-0.11
7:42:17.1	74:12: 4	22.00	0.74	1.08	0.43
7:42:17.5	74:13:40	22.30	0.56	0.95	1.18
7:42:18.1	74:10:22	20.50	2.43	0.91	0.22
7:42:18.9	74:12:37	21.70	1.20	0.66	0.63
7:42:20.7	74:12:35	21.76	–	0.30	0.14
7:42:21.1	74:11:39	22.21	1.88	1.35	1.09
7:42:21.3	74:16: 4	22.76	2.31	1.53	1.66
7:42:21.5	74:15:31	21.67	3.78	0.66	-0.09
7:42:22.1	74:10:17	19.73	2.56	0.86	0.55
7:42:22.8	74:12:45	21.83	1.64	1.22	1.46
7:42:23.6	74:11:32	19.05	1.23	0.73	0.66
7:42:23.7	74:14:13	22.08	1.63	1.24	0.60
7:42:24.0	74:10:13	20.43	4.11	0.75	0.37
7:42:26.6	74:15:36	18.64	0.82	0.53	0.51
7:42:27.3	74:11:18	20.81	0.85	0.77	0.51
7:42:27.4	74:12:50	19.80	1.65	0.85	0.66
7:42:27.5	74:12: 3	19.01	1.55	0.79	0.73
7:42:28.6	74:13:16	19.70	1.52	1.10	1.16
7:42:29.6	74:13:23	18.71	1.79	0.88	0.77
7:42:30.1	74:13:30	20.88	1.25	0.96	0.65
7:42:30.7	74:14:13	20.72	1.66	0.97	0.61
7:42:30.7	74:15:31	20.49	0.89	0.67	0.75
7:42:31.0	74:11:58	20.29	1.27	0.76	0.65
7:42:31.1	74:16:25	21.87	1.37	0.72	0.96
7:42:31.4	74:13:57	22.84	0.90	1.39	1.27
7:42:31.6	74:13: 0	21.97	0.67	0.81	0.14
7:42:32.0	74:12:38	20.90	1.23	1.18	0.67
7:42:33.0	74:16:58	21.09	0.84	0.77	0.20
7:42:33.3	74:11: 2	20.00	1.58	0.82	0.71
7:42:34.0	74:11:38	21.39	1.87	0.94	0.55
7:42:34.6	74:17:51	21.77	1.20	0.51	–
7:42:34.7	74:10:44	22.20	1.64	1.30	1.66
7:42:34.8	74:13:25	21.86	2.17	1.29	1.27
7:42:35.6	74:16:41	21.46	0.65	0.72	0.50

MS0735					contd.
RA(2000)	Dec(2000)	V	B-V	V-R	R-I
7:42:37.3	74:11:12	20.43	1.04	0.51	0.57
7:42:37.8	74:10:33	22.34	1.01	0.89	1.26
7:42:38.0	74:17:16	20.65	0.83	0.68	0.53
7:42:38.3	74:14: 7	19.52	1.27	0.75	0.71
7:42:38.4	74:14:43	22.09	0.76	1.19	1.60
7:42:38.6	74:10:47	21.81	–	1.02	1.66
7:42:38.9	74:15: 2	20.08	1.63	0.90	0.78
7:42:39.6	74:15:21	20.01	1.22	0.59	0.59
7:42:39.7	74:14: 8	21.74	0.51	0.78	0.97
7:42:40.0	74:12: 2	19.59	1.19	0.82	0.76
7:42:40.4	74:12:13	21.24	1.25	1.06	1.09
7:42:42.1	74:16:39	21.54	1.13	1.35	0.90
7:42:43.2	74:10:55	22.04	1.58	1.01	0.32
7:42:43.8	74:15:54	20.85	1.71	0.91	0.95
7:42:44.5	74:11:38	22.00	0.41	1.08	1.07
7:42:46.0	74:16:15	21.93	–	1.05	1.05
7:42:46.1	74:17:51	21.59	1.19	0.40	–
7:42:46.5	74:15:32	19.40	1.62	0.92	0.75
7:42:46.5	74:17:38	22.65	-0.19	1.76	1.64
7:42:46.8	74:14:32	20.79	0.80	0.62	0.76
7:42:47.6	74:10:59	19.99	2.02	0.51	0.98
7:42:48.1	74:11: 4	18.52	1.85	0.85	0.80
7:42:48.5	74:15:47	20.34	0.91	0.67	0.41
7:42:49.0	74: 9:39	20.05	0.63	0.60	0.34
7:42:49.5	74:17:41	21.32	1.56	0.82	-0.41
7:42:49.6	74:11:56	19.94	1.85	0.97	0.74
7:42:50.4	74:11:30	21.47	0.75	0.80	0.28
7:42:51.2	74: 9:46	20.39	1.89	0.72	0.62
7:42:51.8	74:12:43	21.77	–	1.21	1.39
7:42:53.1	74:14:23	21.34	3.01	1.17	1.23
7:42:53.3	74:13:31	22.15	–	1.20	1.17
7:42:54.4	74:12:48	19.03	1.74	1.10	1.20
7:42:54.8	74:14:16	21.12	0.87	0.74	0.45
7:42:54.9	74:14:39	20.64	1.25	0.76	0.56
7:42:55.8	74:11:25	20.34	1.61	0.61	0.78
7:42:55.9	74:10:13	20.31	2.25	0.95	0.71
7:42:57.3	74:12: 5	19.22	1.67	0.90	0.79
7:42:57.9	74:10:49	21.02	0.35	1.07	0.43
7:42:59.2	74:12:45	20.00	–	0.77	0.45
7:42:59.9	74: 9:47	20.33	–	0.93	0.42
7:42:60.0	74:15: 0	19.70	–	0.72	0.42

Table 10. Catalog of galaxies in the field of MS 01306.7−0121.

RA(2000)	Dec(2000)	V	B-V	V-R	R-I
13: 8:57.5	-1:35:14	20.99	1.02	0.75	0.36
13: 8:57.5	-1:36:59	20.94	1.70	0.94	0.20
13: 8:57.8	-1:33:27	19.24	1.32	0.93	0.85
13: 8:57.8	-1:38:18	19.83	1.48	1.20	1.56
13: 8:58.2	-1:35:10	20.50	1.06	1.26	1.46
13: 8:58.2	-1:40:50	20.66	0.27	0.06	0.01
13: 8:58.9	-1:32:25	20.39	1.17	0.34	–
13: 8:58.9	-1:41:46	20.25	0.08	0.39	0.42
13: 8:60.0	-1:39:24	21.20	1.08	1.09	0.64
13: 9: 0.4	-1:37:53	19.28	0.32	0.69	0.24
13: 9: 0.7	-1:36:29	19.31	1.41	1.13	1.16
13: 9: 0.7	-1:36:42	21.24	0.72	1.20	0.44
13: 9: 0.7	-1:39:25	20.30	0.87	0.81	0.48
13: 9: 0.7	-1:41: 0	20.18	0.46	0.43	0.40
13: 9: 1.1	-1:34:54	20.81	1.25	1.49	1.57
13: 9: 1.1	-1:41:24	20.38	1.22	1.17	1.61
13: 9: 1.4	-1:36:50	21.09	0.72	1.60	1.05
13: 9: 1.4	-1:40: 5	20.55	1.26	0.42	0.43
13: 9: 2.5	-1:34:13	20.57	0.30	0.74	0.87
13: 9: 2.5	-1:37:37	20.13	0.51	0.88	0.44
13: 9: 2.9	-1:34:40	18.75	1.08	0.80	0.64
13: 9: 3.2	-1:39:11	24.56	-2.20	4.03	1.80
13: 9: 3.6	-1:40: 8	21.20	0.19	1.17	0.96
13: 9: 3.6	-1:41:57	19.38	1.13	0.65	0.91
13: 9: 4.3	-1:31:59	19.84	1.28	0.17	–
13: 9: 4.7	-1:37:17	19.90	0.15	0.62	0.73
13: 9: 5.0	-1:31:56	18.03	1.65	0.96	–
13: 9: 5.0	-1:36:22	20.35	0.54	0.95	0.95
13: 9: 5.0	-1:36:43	16.96	0.73	0.43	0.69
13: 9: 5.4	-1:35:59	21.29	0.35	0.96	1.20
13: 9: 5.8	-1:34:18	22.75	0.79	2.53	1.51
13: 9: 5.8	-1:37:49	22.20	-0.66	2.03	0.91
13: 9: 6.1	-1:33:29	20.83	2.07	1.18	1.23
13: 9: 6.1	-1:33:53	18.28	1.36	0.78	0.86
13: 9: 6.5	-1:35: 8	19.34	0.83	0.72	0.94
13: 9: 6.5	-1:38: 5	19.20	0.48	0.65	0.45
13: 9: 6.5	-1:38:21	19.31	1.05	0.86	0.72
13: 9: 6.8	-1:34:35	19.45	0.82	0.84	0.75
13: 9: 7.2	-1:37: 1	19.38	1.16	0.98	0.94
13: 9: 7.2	-1:40:42	21.58	0.01	0.83	0.13
13: 9: 7.6	-1:35:39	17.00	0.62	0.42	0.71
13: 9: 7.6	-1:38:38	19.27	0.98	0.82	0.62
13: 9: 7.6	-1:41:15	18.67	1.22	0.81	0.60
13: 9: 7.9	-1:37:15	17.06	1.13	0.67	0.83
13: 9: 8.3	-1:39: 5	20.85	-0.28	1.03	-0.27
13: 9: 8.3	-1:42:14	20.61	0.66	0.77	0.01
13: 9: 8.6	-1:32:15	19.24	0.82	0.31	–
13: 9: 8.6	-1:39:59	19.99	0.73	0.80	0.36
13: 9: 9.0	-1:33:41	18.51	1.06	0.74	0.81
13: 9: 9.0	-1:34:52	20.17	1.64	1.29	1.03
13: 9: 9.4	-1:34:29	22.03	-0.32	2.15	1.38
13: 9: 9.4	-1:39:53	22.44	-0.14	2.06	0.12
13: 9: 9.4	-1:40:12	20.60	0.80	0.78	-0.08
13: 9: 9.7	-1:32: 9	16.38	1.25	0.67	–
13: 9: 9.7	-1:34:31	23.42	-0.31	3.31	1.55
13: 9: 9.7	-1:36:25	18.31	1.02	0.74	0.75
13: 9: 9.7	-1:36:59	16.49	1.87	-0.37	1.15
13: 9:10.1	-1:33:38	20.72	1.34	1.63	1.28
13: 9:10.1	-1:34: 9	20.56	1.39	1.74	1.16
13: 9:10.4	-1:33:23	19.51	0.98	0.58	0.80
13: 9:10.4	-1:33:44	22.01	1.36	2.03	1.32
13: 9:11.2	-1:36: 4	20.86	0.92	1.11	1.17
13: 9:11.2	-1:41: 7	21.18	1.50	1.31	-0.57
13: 9:11.5	-1:33:52	20.16	0.86	0.84	0.90
13: 9:11.5	-1:39:41	20.91	0.89	1.21	0.57
13: 9:11.5	-1:42: 3	21.97	-0.06	1.61	-0.26

MS1306					contd.
RA(2000)	Dec(2000)	V	B-V	V-R	R-I
13: 9:11.9	-1:38:35	20.97	0.80	0.92	0.42
13: 9:12.2	-1:36:18	20.98	1.29	1.18	0.85
13: 9:12.6	-1:38:52	21.47	1.19	1.71	0.71
13: 9:12.6	-1:39:56	22.05	0.04	1.65	-0.64
13: 9:13.0	-1:36:15	21.16	1.75	1.72	1.12
13: 9:13.3	-1:35:47	23.50	-0.37	3.06	1.39
13: 9:13.3	-1:36: 7	17.88	1.14	0.71	0.84
13: 9:13.7	-1:35: 1	21.91	1.56	2.10	1.27
13: 9:13.7	-1:36:48	20.14	0.83	0.91	0.93
13: 9:13.7	-1:39: 3	19.42	1.08	0.89	0.59
13: 9:14.0	-1:36:33	16.89	1.20	0.66	0.85
13: 9:14.4	-1:32:52	21.29	0.20	0.91	1.19
13: 9:14.4	-1:33:12	21.36	0.07	0.75	1.44
13: 9:14.4	-1:41:38	21.57	-0.24	1.19	-0.77
13: 9:14.8	-1:39:15	22.03	0.94	1.61	0.51
13: 9:15.1	-1:34: 8	21.67	0.16	1.39	1.04
13: 9:15.5	-1:32:28	19.51	1.69	1.09	–
13: 9:15.8	-1:35:56	17.25	1.18	0.69	0.86
13: 9:15.8	-1:41:55	21.26	0.28	1.15	-0.17
13: 9:16.2	-1:34:30	17.09	1.20	0.69	0.88
13: 9:16.9	-1:38:22	20.52	1.53	1.11	1.56
13: 9:16.9	-1:40:26	19.07	1.71	1.13	0.82
13: 9:17.3	-1:37: 7	19.99	0.89	0.82	1.19
13: 9:17.6	-1:33:23	19.91	1.17	1.19	0.88
13: 9:17.6	-1:34: 5	21.53	0.04	1.53	0.81
13: 9:17.6	-1:36:54	16.34	1.22	0.63	0.87
13: 9:17.6	-1:39: 1	20.75	0.66	0.82	0.85
13: 9:18.0	-1:33:15	21.20	0.39	1.10	0.83
13: 9:18.0	-1:41:32	20.62	0.97	1.17	0.45
13: 9:18.4	-1:42:12	21.73	0.87	1.52	0.57
13: 9:19.1	-1:32:52	18.14	0.91	0.66	0.78
13: 9:19.1	-1:34:17	19.31	0.93	0.95	0.77
13: 9:19.1	-1:34:53	20.16	0.68	0.95	0.81
13: 9:19.1	-1:36: 9	19.81	1.01	0.64	1.06
13: 9:19.1	-1:37: 9	17.71	1.28	0.29	1.09
13: 9:19.1	-1:37:22	14.89	1.24	0.62	0.86
13: 9:19.1	-1:38:22	19.87	1.16	0.67	0.94
13: 9:19.1	-1:38:30	20.06	1.58	0.78	0.87
13: 9:19.4	-1:37:49	19.89	1.24	0.30	1.35
13: 9:19.4	-1:39:41	19.06	0.87	0.76	0.50
13: 9:19.4	-1:41:33	19.22	1.19	0.83	0.67
13: 9:19.8	-1:37:37	19.35	1.05	0.47	1.00
13: 9:19.8	-1:37:43	20.01	0.92	0.50	1.52
13: 9:20.2	-1:35:46	20.01	1.13	1.12	1.02
13: 9:20.2	-1:36:17	16.56	1.18	0.63	0.89
13: 9:20.2	-1:42: 9	20.69	1.64	1.11	1.14
13: 9:20.5	-1:32:12	20.31	0.84	0.03	–
13: 9:20.5	-1:32:42	20.85	0.81	0.27	-0.79
13: 9:20.5	-1:34:56	18.15	0.53	0.39	0.58
13: 9:20.5	-1:35: 7	17.75	1.11	0.65	0.83
13: 9:20.5	-1:37:34	20.02	1.00	0.55	1.07
13: 9:20.5	-1:42:12	20.48	1.14	0.68	0.34
13: 9:20.9	-1:37:24	17.99	1.13	0.67	0.85
13: 9:20.9	-1:40:31	19.90	0.79	0.97	0.41
13: 9:20.9	-1:42:10	20.29	0.76	0.72	0.25
13: 9:20.9	-1:42:20	19.57	1.27	0.68	0.66
13: 9:21.2	-1:37:59	16.98	1.18	0.63	0.86
13: 9:21.2	-1:42: 4	18.91	1.33	0.73	0.70
13: 9:21.6	-1:38:28	18.80	1.16	0.79	0.71
13: 9:21.6	-1:39:52	19.99	0.61	1.02	0.56
13: 9:21.6	-1:40:58	18.98	1.07	0.91	0.56
13: 9:22.0	-1:34:47	20.16	1.40	1.16	0.90
13: 9:22.3	-1:37: 6	20.31	0.26	0.51	0.74
13: 9:22.3	-1:38:52	19.89	0.46	0.85	0.40
13: 9:22.3	-1:39:42	21.36	-0.01	1.21	-0.18
13: 9:23.0	-1:36:18	20.76	0.43	0.87	0.83

MS1306					contd.
RA(2000)	Dec(2000)	V	B-V	V-R	R-I
13: 9:23.0	-1:36:39	21.12	0.06	0.93	0.92
13: 9:23.4	-1:32:26	19.47	1.54	0.56	–
13: 9:23.4	-1:34:18	21.30	0.44	1.30	0.91
13: 9:23.4	-1:35:50	22.31	-0.44	1.87	1.23
13: 9:23.4	-1:40:49	21.08	1.44	1.38	0.40
13: 9:23.8	-1:33:35	18.98	1.06	0.74	0.64
13: 9:23.8	-1:33:44	19.84	0.97	0.76	0.44
13: 9:23.8	-1:34:12	21.04	1.01	0.92	0.24
13: 9:24.1	-1:33:46	19.69	0.90	0.74	0.43
13: 9:24.1	-1:36:36	22.84	-0.35	2.69	1.51
13: 9:24.1	-1:38:43	19.86	0.97	0.94	0.54
13: 9:24.1	-1:41:29	20.90	0.79	1.03	-0.81
13: 9:24.5	-1:39: 1	21.27	0.11	1.31	0.05
13: 9:24.5	-1:40:53	20.46	1.39	1.46	0.68
13: 9:24.8	-1:32:38	16.42	0.98	0.64	–
13: 9:24.8	-1:34:46	19.78	0.88	0.34	0.28
13: 9:24.8	-1:36:42	19.08	0.88	0.81	0.60
13: 9:24.8	-1:36:56	18.15	1.06	0.70	0.76
13: 9:25.2	-1:32:59	20.63	1.04	0.58	0.99
13: 9:25.9	-1:33:59	19.11	0.78	0.56	0.36
13: 9:26.6	-1:34:22	17.24	1.18	0.63	0.82
13: 9:26.6	-1:40: 8	21.61	1.56	1.86	0.21
13: 9:26.6	-1:40:41	20.06	0.58	0.89	0.00
13: 9:27.4	-1:32:50	16.84	1.27	0.63	0.82
13: 9:27.4	-1:34: 5	20.81	1.15	0.67	0.10
13: 9:27.4	-1:37:55	17.68	1.13	0.65	0.76
13: 9:27.4	-1:38: 0	18.61	1.11	0.67	0.63
13: 9:27.4	-1:41:20	21.29	1.08	–	–
13: 9:27.7	-1:32:33	20.50	1.94	0.32	–
13: 9:27.7	-1:36:29	20.42	0.69	0.74	-0.03
13: 9:27.7	-1:38:19	21.71	-0.30	1.58	0.04
13: 9:28.1	-1:36:25	21.03	0.89	0.81	-0.89
13: 9:28.1	-1:37:50	20.01	1.05	0.97	0.31
13: 9:28.1	-1:39:23	17.84	1.07	0.67	0.73
13: 9:28.8	-1:33: 9	20.46	3.20	0.64	1.09
13: 9:28.8	-1:37:23	19.58	1.10	0.87	0.43
13: 9:29.2	-1:32: 5	20.36	1.96	-0.11	–
13: 9:29.5	-1:33:21	19.93	2.75	-0.17	-0.27
13: 9:29.9	-1:32:29	20.33	2.29	-0.25	–
13: 9:29.9	-1:33:20	20.55	1.55	-0.04	–
13: 9:29.9	-1:36: 0	20.69	2.60	0.95	0.96
13: 9:29.9	-1:36:32	20.90	0.72	0.87	-1.10
13: 9:29.9	-1:38:46	22.52	-0.51	1.89	–
13: 9:30.2	-1:35: 9	17.89	1.23	0.63	0.73
13: 9:30.2	-1:38:20	18.40	1.08	0.70	0.70
13: 9:30.2	-1:42: 2	20.31	1.05	0.28	-0.06
13: 9:30.6	-1:37:46	20.34	0.66	0.59	-0.75
13: 9:30.6	-1:37:51	18.78	0.40	0.40	0.12
13: 9:30.6	-1:38:21	17.98	1.48	0.92	1.05
13: 9:31.0	-1:37:22	23.70	-0.09	3.20	0.14
13: 9:31.3	-1:32:57	19.66	2.98	0.65	0.16
13: 9:31.3	-1:38:52	19.07	1.35	0.56	0.68
13: 9:31.3	-1:39: 3	18.76	1.01	0.54	0.53
13: 9:31.7	-1:34:53	20.37	1.45	0.99	0.79
13: 9:31.7	-1:35:34	20.21	1.34	0.40	0.34
13: 9:31.7	-1:36:50	19.85	1.07	0.76	0.17
13: 9:32.0	-1:32: 9	20.23	1.71	-0.27	–
13: 9:32.0	-1:37:36	20.52	1.78	1.15	0.16
13: 9:32.0	-1:41:50	21.37	2.54	1.10	-0.61
13: 9:32.4	-1:34:38	17.18	1.29	0.66	0.80
13: 9:32.8	-1:36:33	20.78	3.96	1.00	0.92
13: 9:32.8	-1:36:59	20.52	1.11	0.57	-0.93
13: 9:33.1	-1:36:34	21.15	4.01	1.05	-0.60
13: 9:33.1	-1:37: 0	21.38	–	1.11	-0.43
13: 9:33.1	-1:38:45	17.93	0.02	-0.07	-0.01
13: 9:33.5	-1:33:57	20.54	2.07	-0.27	–

MS1306					contd.
RA(2000)	Dec(2000)	V	B-V	V-R	R-I
13: 9:33.5	-1:34:53	16.99	1.24	0.63	0.81
13: 9:33.5	-1:35:35	19.05	1.18	0.62	0.49
13: 9:33.5	-1:40:45	20.02	1.85	1.38	2.14
13: 9:33.8	-1:41:59	20.35	1.70	–	-0.32
13: 9:34.2	-1:34:23	20.41	2.26	0.12	–
13: 9:34.6	-1:38:37	21.26	1.72	0.63	–
13: 9:34.6	-1:40:39	19.20	0.92	0.43	-0.05
13: 9:34.9	-1:33:23	19.24	1.48	0.45	-0.57
13: 9:34.9	-1:37:35	20.58	1.01	0.40	–
13: 9:35.3	-1:35: 1	20.33	2.49	0.22	–
13: 9:35.3	-1:37: 0	19.95	1.04	0.35	-1.29
13: 9:35.3	-1:38:11	19.50	1.87	0.94	0.91
13: 9:35.6	-1:40:22	20.37	1.18	–	-0.32
13: 9:36.0	-1:33: 4	18.02	0.98	0.44	–
13: 9:36.0	-1:35:33	19.55	1.72	0.64	–
13: 9:36.4	-1:39:56	20.14	2.12	0.33	–
13: 9:36.7	-1:34:34	19.97	1.97	0.63	–
13: 9:36.7	-1:38: 4	21.19	0.98	0.62	–
13: 9:36.7	-1:41:50	18.66	0.65	0.40	–
13: 9:37.1	-1:37: 2	20.05	1.35	0.14	–
13: 9:37.4	-1:38:18	19.50	1.21	0.32	–
13: 9:37.8	-1:36:12	19.76	1.51	-0.03	–
13: 9:37.8	-1:38:27	20.38	2.23	-0.04	–
13: 9:38.2	-1:35:19	19.77	2.00	-0.23	–
13: 9:38.2	-1:35:35	20.12	1.66	0.05	–
13: 9:38.2	-1:36: 0	17.55	0.89	0.50	–
13: 9:38.5	-1:38:25	18.49	1.21	0.54	–
13: 9:38.5	-1:38:32	20.23	1.98	–	-0.32
13: 9:38.5	-1:41:39	18.64	0.71	0.33	–
13: 9:38.9	-1:36:54	19.04	0.96	0.27	–
13: 9:39.2	-1:38: 2	19.28	1.09	0.10	–